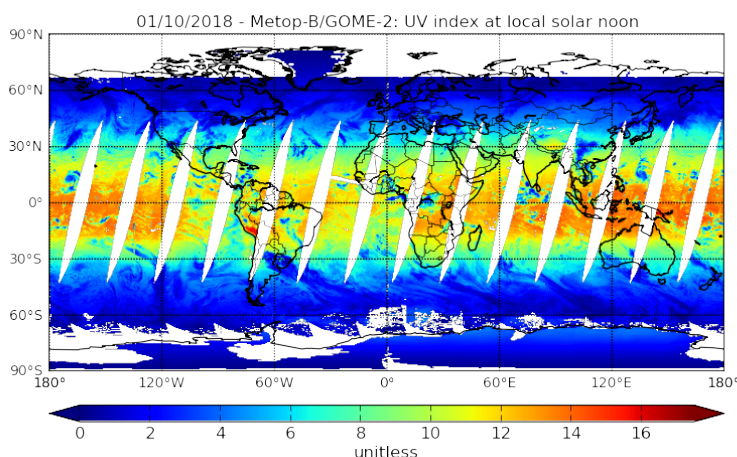


AC SAF VALIDATION REPORT

Validated products:

Name; ID	Satellite(s)
UV Data record R1 O3M-138 – O3M-152: daily dose, daily maximum dose rate, UV index	Merged Metop-A/B
Offline UV product version 2 O3M-450 – O3M-464: daily dose, UV index	



Author:

Name	Institute
Kaisa Lakkala, Niilo Kalakoski, Jukka Kujanpää	Finnish Meteorological Institute

Reporting period: June 2007 – May 2017

Input data versions: OTO/O3 version GDP 4.8
 MetOp-A AVHRR L1b GAC version 1.0, 01/06/2007 - 31/05/2013
 MetOp-B AVHRR L1b GAC version 1.0, 31/03/2013 - 31/05/2017
 N-18 AVHRR L1b GAC version 1.0, 01/06/2007 - 30/06/2009
 N-19 AVHRR L1b GAC version 1.0, 30/06/2009 - 31/05/2017

Data processor versions: Offline UV product version 1: 1.13, 01/06/2007 - 09/07/2013
 1.20, 09/07/2013 - 31/05/2017
 Offline UV product version 2: 2.20, 01/06/2016 - 31/05/2017
 UV Data Record R1: 2.20, 01/06/2007 - 31/05/2017

Introduction to EUMETSAT Satellite Application Facility on Atmospheric Composition monitoring (AC SAF)

Background

The monitoring of atmospheric chemistry is essential due to several human caused changes in the atmosphere, like global warming, loss of stratospheric ozone, increasing UV radiation, and pollution. Furthermore, the monitoring is used to react to the threats caused by the natural hazards as well as follow the effects of the international protocols.

Therefore, monitoring the chemical composition and radiation of the atmosphere is a very important duty for EUMETSAT and the target is to provide information for policy makers, scientists and general public.

Objectives

The main objectives of the AC SAF is to process, archive, validate and disseminate atmospheric composition products (O₃, NO₂, SO₂, BrO, HCHO, H₂O, OClO, CO, NH₃), aerosol products and surface ultraviolet radiation products utilising the satellites of EUMETSAT. The majority of the AC SAF products are based on data from the GOME-2 and IASI instruments onboard Metop satellites.

Another important task besides the near real-time (NRT) and offline data dissemination is the provision of long-term, high-quality atmospheric composition products resulting from reprocessing activities.

Product categories, timeliness and dissemination

NRT products are available in less than three hours after measurement. These products are disseminated via EUMETCast, WMO GTS or internet.

- Near real-time trace gas columns (total and tropospheric O₃ and NO₂, total SO₂, total HCHO, CO) and high-resolution ozone profiles
- Near real-time absorbing aerosol indexes from main science channels and polarization measurement detectors
- Near real-time UV indexes, clear-sky and cloud-corrected

Offline products are available within two weeks after measurement and disseminated via dedicated web services at EUMETSAT and AC SAF.

- Offline trace gas columns (total and tropospheric O₃ and NO₂, total SO₂, total BrO, total HCHO, total H₂O) and high-resolution ozone profiles
- Offline absorbing aerosol indexes from main science channels and polarization measurement detectors
- Offline surface UV, daily doses and daily maximum values with several weighting functions

Data records are available after reprocessing activities from the EUMETSAT Data Centre and/or the AC SAF archives.

- Data records generated in reprocessing
- Lambertian-equivalent reflectivity
- Total OClO

Users can access the AC SAF offline products and data records (free of charge) by registering at the AC SAF web site.

More information about the AC SAF project, products and services: <https://acsaf.org/>

AC SAF Helpdesk: helpdesk@acsaf.org

Twitter: https://twitter.com/Atmospheric_SAF

Document change log

Issue	Date	Modified items
1/2018 draft	17.12.2018	Initial version
1/2019	19.2.2019	Updated according to RIDS and subsequent discussions. Added explanation of the adopted validation scheme. Added comments on the results against the service specification accuracy threshold. Added a map showing the validation sites.

Contents

1	Introduction	1
1.1	Purpose and scope	1
1.2	Acronyms	1
1.3	References	2
1.3.1	Applicable Documents	2
1.3.2	Reference Documents	2
2	Data sources	3
2.1	Offline operational v1 UV product	3
2.2	UV Data record and offline operational v2 UV products	3
2.3	Ground based measurements	12
3	Validation results	14
3.1	Comparison with ground based measurements	14
3.2	Differences between OUV OPER v1 and OUV RECO	25
3.3	Differences between OUV OPER v2 and OUV RECO	32
4	Conclusions	39
5	Acknowledgments	40
	Appendices	41

Chapter 1

Introduction

1.1 Purpose and scope

The purpose of this document is to present the validation of EUMETSAT Satellite Application Facility on Atmospheric Composition Monitoring (AC SAF) UV Data Record R1 products (OUV RECO), specifically compare the data record product with the actual reference offline operational UV product version 1 (OUV OPER v1) and ground based measurements for the period 2007-2017. In addition, the offline operational UV product version 2 (OUV OPER v2) is compared with OUV RECO for the period 1 June 2016 – 31 May 2017.

1.2 Acronyms

ARPA-VDA	Agenzia Regionale per la Protezione dell’Ambiente Valle d’Aosta
AUTH	Aristotle University of Thessaloniki
ATBD	Algorithm Theoretical Basis Document
CIE	Commission Internationale de L’Eclairage, International Commission on Illumination
HKPU	Hong Kong Polytechnic University
EUMETSAT	European Organisation for the Exploitation of Meteorological Satellites
FMI	Finnish Meteorological Institute
GOME	Global Ozone Monitoring Experiment
IEM-SPA	The Institute of Experimental Meteorology Scientific & Production Association
IAO	V.E. Zuev Institute of Atmospheric Optic
JMA	Japan Meteorological Agency
AC SAF	Satellite Application Facility on Atmospheric Composition Monitoring
MSC	Meteorological Service of Canada
NEUBrew	NOAA-EPA Brewer UV and Ozone Network - NEUBrew
NSF	National Science Foundation
RAS-IAP	Obukhov Institute of Atmospheric Physics Russian Academy of Sciences
RMIB	Royal Meteorological Institute of Belgium
U. Toronto	University of Toronto
OUV OPER v1	Offline operational UV product version 1
OUV OPER v2	Offline operational UV product version 2
OUV RECO	UV Data Record product
PMOD-WRC	Physikalisch-Meteorologisches Observatorium Davos / World Radiation Center
WOUDC	World Ozone and Ultraviolet Radiation Data Centre

1.3 References

1.3.1 Applicable Documents

- [AD1] OUV Algorithm Theoretical Basis Document, SAF/O3M/FMI/ATBD/001, Issue 1.4, 28.6.2013. Kujanpää, J.
- [AD2] OUV Products User Manual, SAF/O3M/FMI/PUM/001, Issue 1.5, 28.6.2013.
- [AD3] OUV Algorithm Theoretical Basis Document, SAF/O3M/FMI/ATBD/001, Issue 2.1, 15.1.2018. Kujanpää, J.
- [AD4] OUV Products User Manual, SAF/AC/FMI/PUM/001, Issue 2.0, 30.11.2018.
- [AD5] O3M SAF Product Requirements Document, Hovila, J., S. Kiemle, O. Tuinder, H. Joench-Soerensen, F. Karcher

1.3.2 Reference Documents

- [RD1] Zaveri, R.A, Shaw, W.J. and Cziczo, D.J., "CARES: Carbonaceous Aerosol and Radiative Effects Study Science Plan", May 2010, DOE/SC-ARM-10-017, <http://www.arm.gov/publications/programdocs/doe-sc-arm-10-017.pdf?id=65>
- [RD2] Commission Internationale de l'Eclairage, 1998, Erythema reference action spectrum and standard erythema dose, CIE S007/E-1998. CIE Central Bureau, Vienna, Austria

Chapter 2

Data sources

2.1 Offline operational v1 UV product

The OUV OPER v1 includes daily doses and maximum dose rates of UV-B and UV-A radiation together with values obtained by different biological weighting functions, solar noon UV index and quality control flags. The OUV products are derived from AC SAF near real-time total ozone column product (NTO/O3) and Advanced Very High Resolution Radiometer (AVHRR) reflectances, therefore combining data from two different instruments onboard the Metop satellite. Sampling of the diurnal cloud cycle is improved by using additional AVHRR data from the NOAA satellites, available through the data exchange between EUMETSAT and NOAA [AD1, AD2].

The algorithm version 1.13 and 1.20 are used for the time periods 1.6.2007–8.7.2013 and 9.7.2013–31.12.2017, correspondingly.

2.2 UV Data record and offline operational v2 UV products

The OUV RECO time series is processed using uniform algorithm version 2.2 throughout the 10-year period [AD3]. The OUV RECO products are derived from AC SAF total column ozone data record, algorithm version 4.8. The UV processor combines observations from GOME-2/Metop-A and GOME-2/Metop-B for better spacial coverage than OUV OPER. The most important differences between OUV RECO and OUV OPER processors are that climatological aerosol optical thickness and surface UV albedo inputs are changed from climatological values to actual daily values. The aerosol optical thickness input of OUV RECO is from Level-3 MODIS Atmosphere Daily Global Product Collection 6, Aqua (MYD08_D3) and Terra (MOD08_D3), Aerosol Optical Depth Land and Ocean. The surface UV albedo input is the Surface Reflectance Daily L3 Global 0.05° CMG collection 6, in which both Aqua (MYD09CMG) and Terra (MOD09CMG) products are used, and band 1=645 nm, band 3=470 nm. The surface pressure input is from ECMWF/ERA-Interim.

The OUV OPER v2 is processed using the same algorithm version than OUV RECO, but aerosol optical thickness, surface UV albedo and surface pressure are taken from a day-of-year climatology [AD3]. The climatology includes mean and standard deviation of these quantities computed for each day of year from the 10-year time series.

OUV RECO and OUV OPER v2 products include same UV products as OUV OPER v1 [AD4]. Here below are examples of OUV RECO and OUV OPER v1 products for one single day and their relative differences. The relative differences shown in Figures 2.2 – 2.7 are almost identical as daily dose products differ from each other only by the chosen action spectrum.

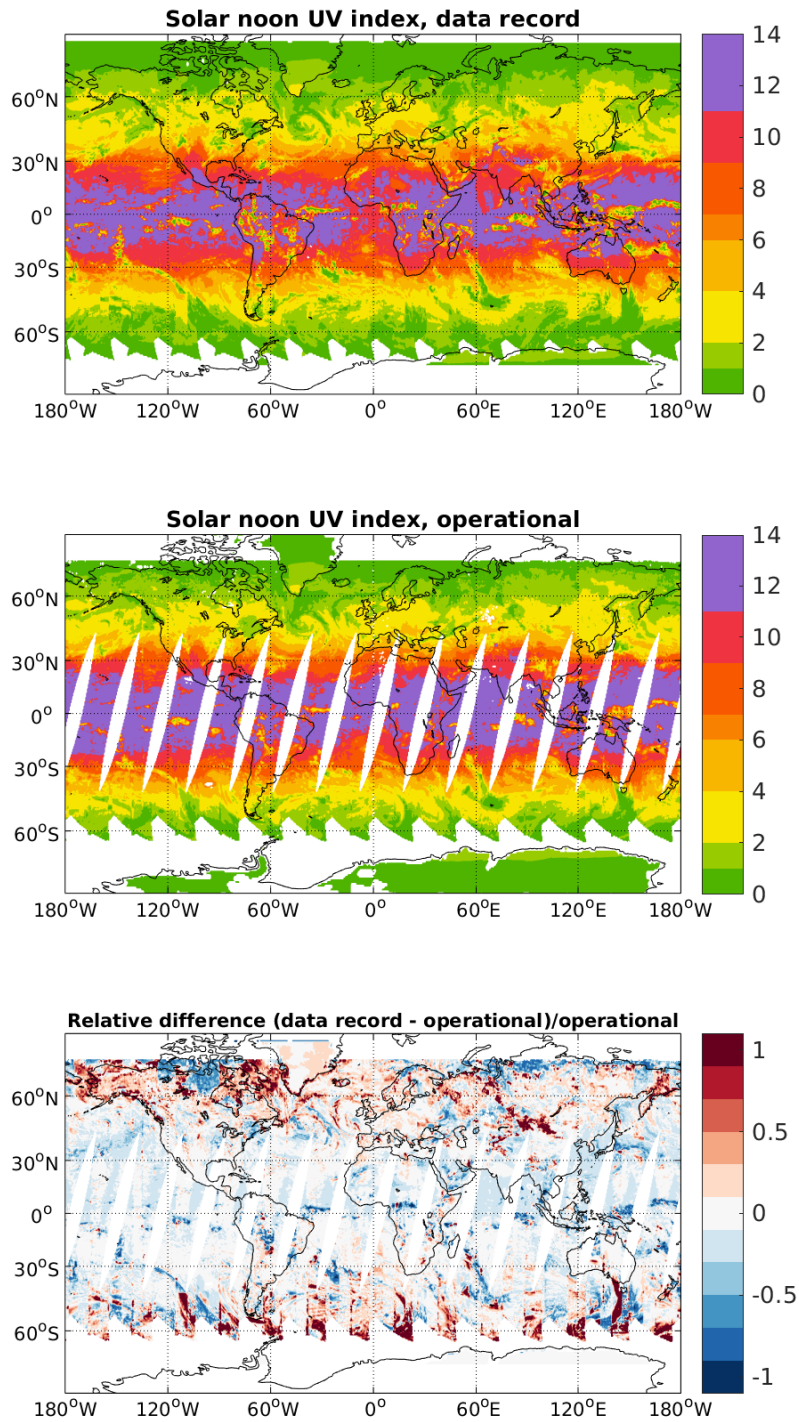


Figure 2.1: Solar noon UV index for 5.3.2017. OUV RECO (top), OUV OPER v1 (second) and relative difference (bottom).

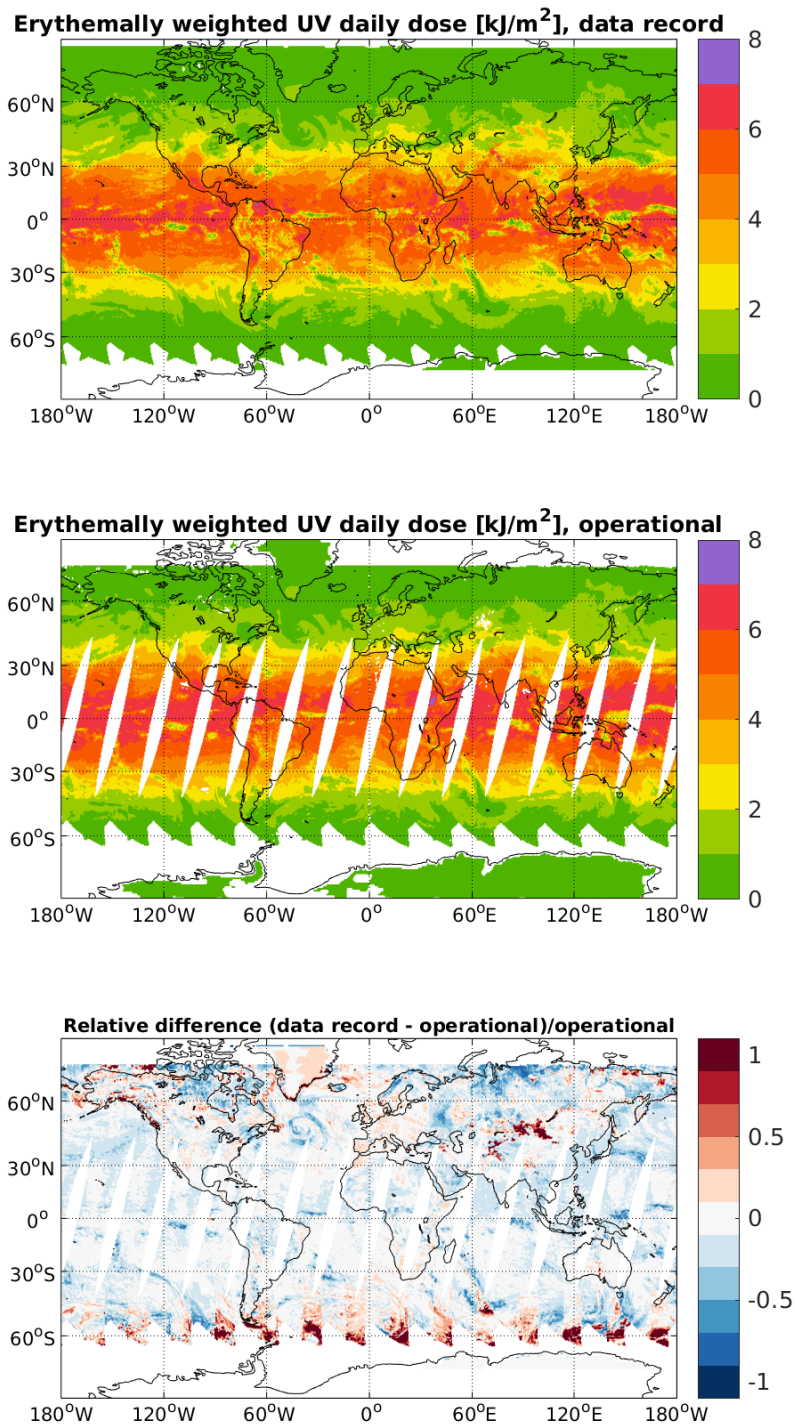


Figure 2.2: Erythemally weighted UV daily doses for 5.3.2017. OUV RECO (top), OUV OPER v1 (second) and relative difference (bottom).

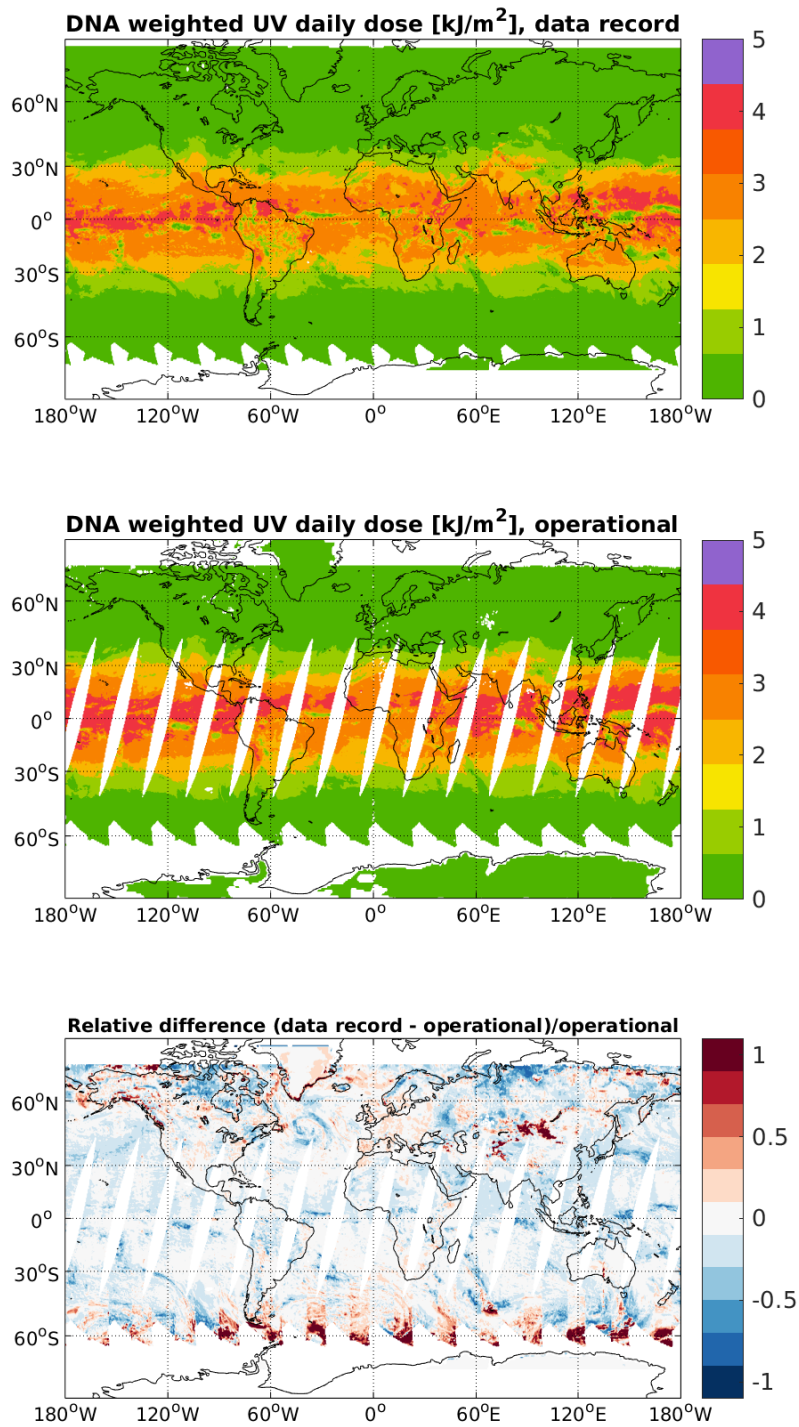


Figure 2.3: DNA weighted UV daily doses for 5.3.2017. OUV RECO (top), OUV OPER v1 (second) and relative difference (bottom).

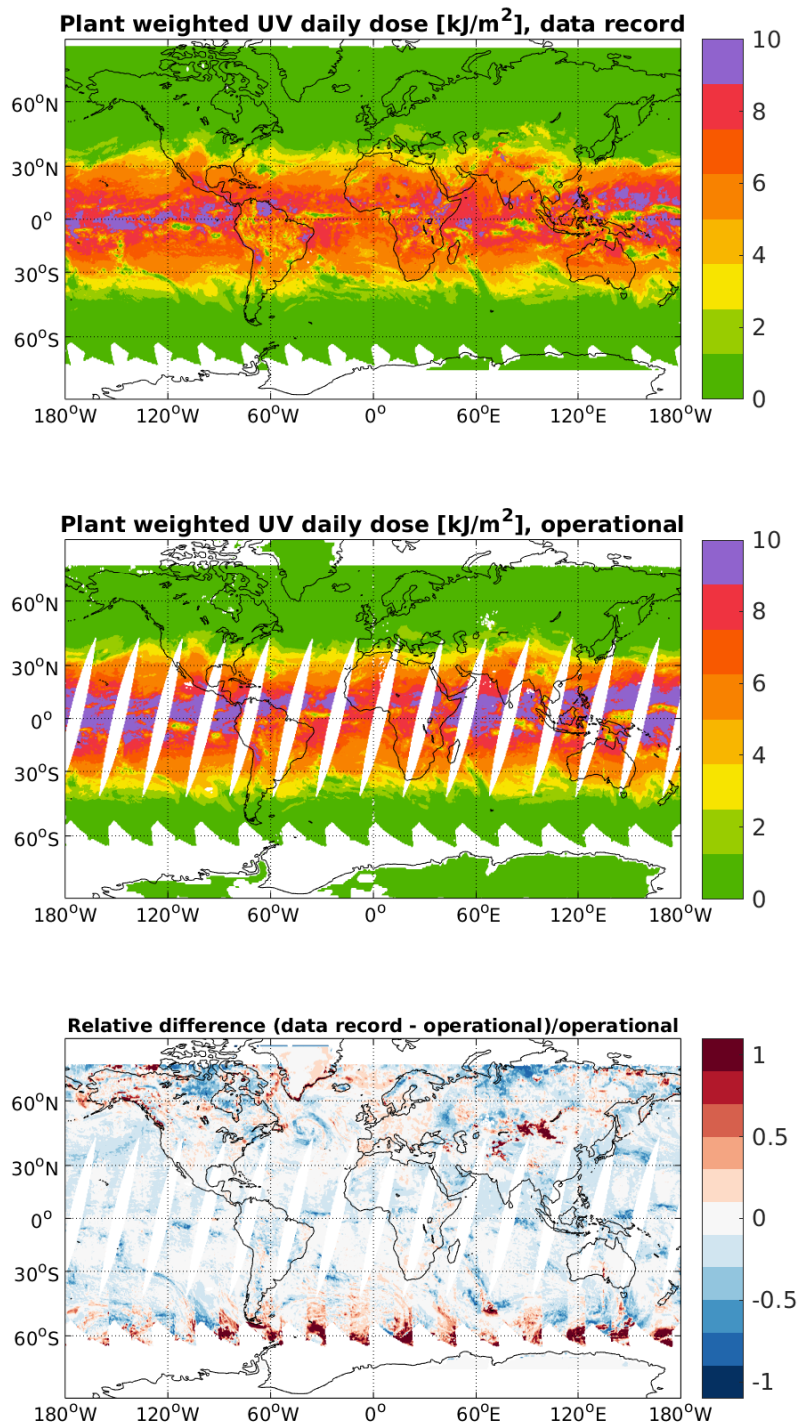


Figure 2.4: UV daily doses weighted with the Plant action spectrum for 5.3.2017. OUV RECO (top), OUV OPER v1 (second) and relative difference (bottom).

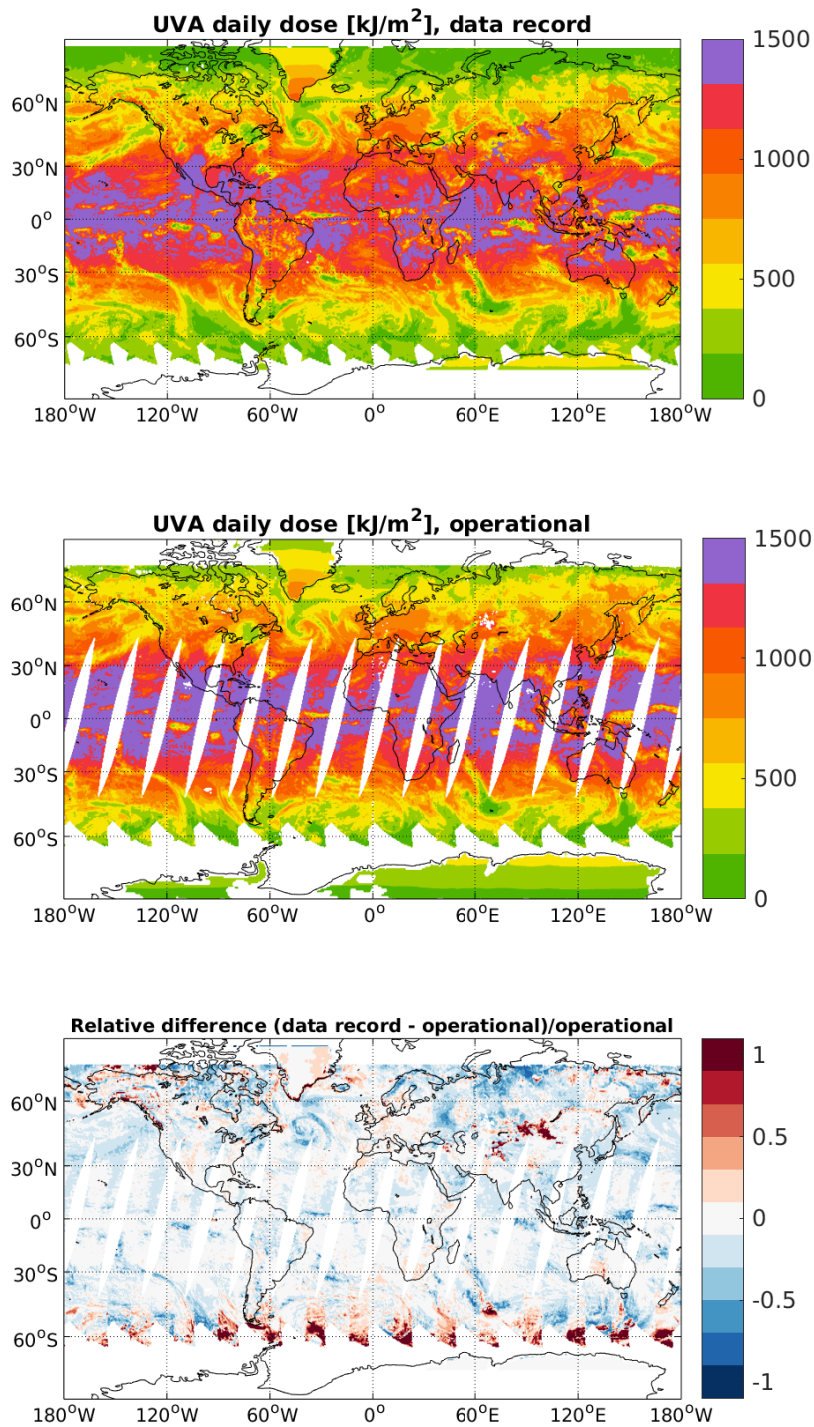


Figure 2.5: UVA daily doses for 5.3.2017. OUV RECO (top), OUV OPER v1 (second) and relative difference (bottom).

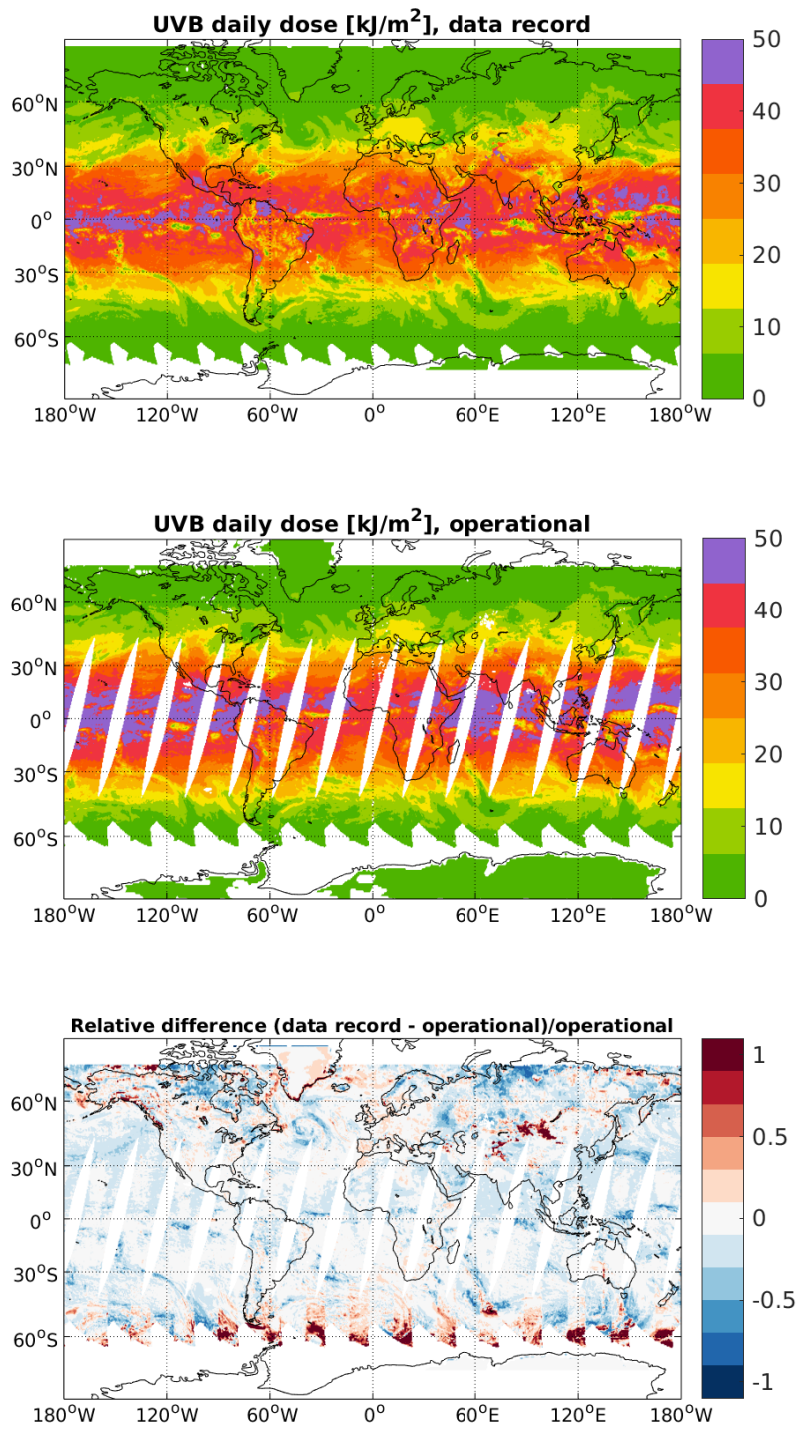


Figure 2.6: UVB daily doses for 5.3.2017. OUV RECO (top), OUV OPER v1 (second) and relative difference (bottom).

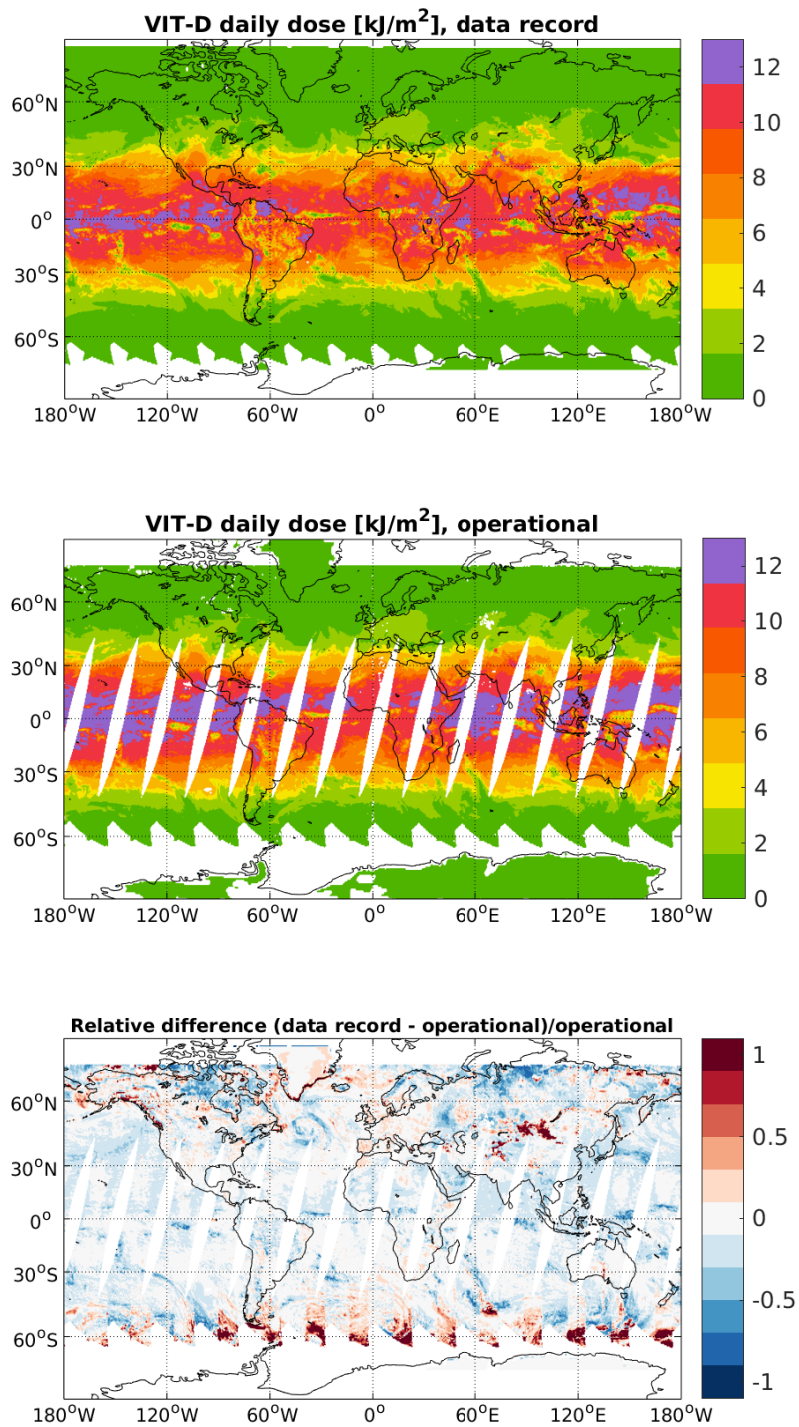


Figure 2.7: UV daily doses weighted with the vitamin D action spectrum for 5.3.2017. OUV RECO (top), OUV OPER v1 (second) and relative difference (bottom).

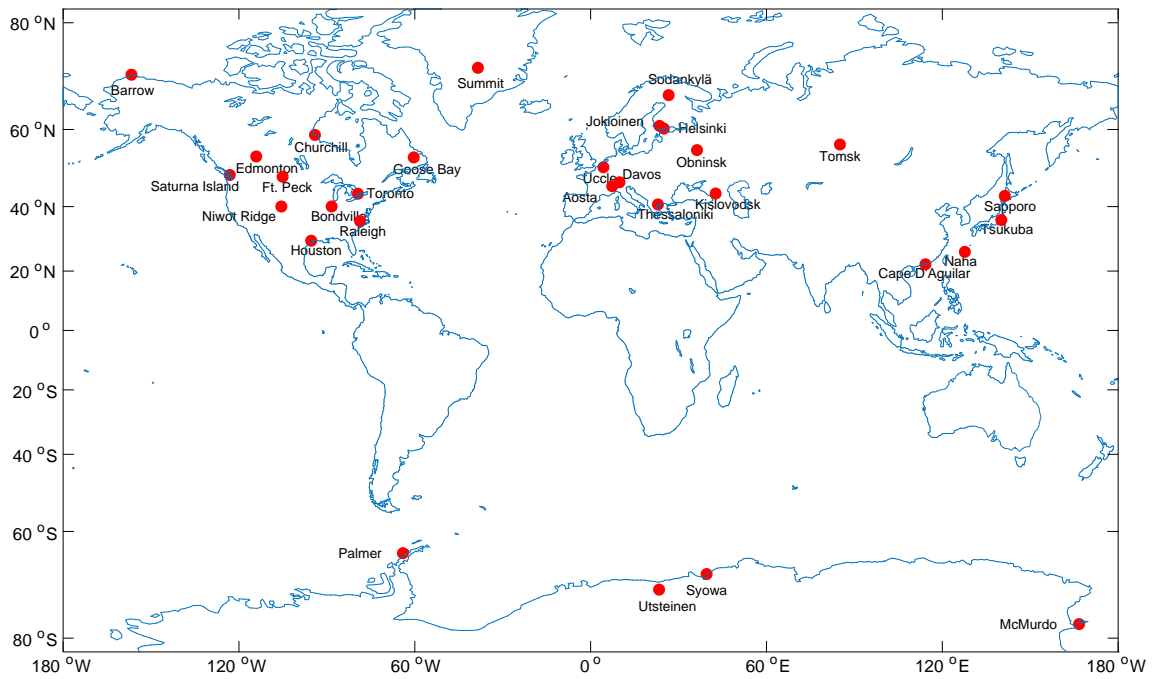


Figure 2.8: Location of the validation sites.

2.3 Ground based measurements

High quality spectroradiometer measurements were used to validate the satellite UV products. Brewer spectroradiometers were used in all stations except at the stations of NSF, in which SUV-spectroradiometers, version 2 data, were used. The stations, their affiliation, instrument, coordinates and elevation are listed in Table 2.1 and their location is showed in Figure 2.8. The data of Sapporo, Tsukuba, Edmonton, Uccle, Toronto, Goose Bay, Churchill, Syowa, Naha, Kislovodsk, Saturna Island, Obninsk, Cape d. Aguilar, Aosta, Tomsk, Utsteinen, Davos and Toronto was downloaded from the WOUDC. The data of Ft. Peck, MRS Niwot Ridge, Raleigh, Bondville and Houston was downloaded from the NEUBrew network. The data of Thessaloniki was provided by AUTH and the data of Jokioinen, Helsinki and Sodankylä by FMI.

Table 2.1: Validation sites

Site	Affiliation	Instruments	Lat., °N	Long., °E	Elev., m
Summit	NSF	SUV-150B	72.58	-38.46	3202
Barrow	NSF	SUV-100	71.32	-156.68	8
Sodankylä	FMI	Brewer Mk II 037	67.37	26.63	179
Jokioinen	FMI	Brewer Mk III 107	60.81	23.50	107
Helsinki	FMI	Brewer Mk III 107	60.20	24.96	50
Churchill	MSC	Brewer Mk II 026, Mk IV 032	58.74	-94.07	35
Tomsk	IAO	Brewer Mk IV 049	56.48	85.07	170
Obninsk	IEM-SPA	Brewer Mk II 044	55.12	36.30	100
Edmonton	MSC	Brewer Mk IV 022, Mk II 055	53.55	-114.10	766
Goose Bay	MSC	Brewer Mk IV 079	53.31	-60.36	40
Uccle	RMIB	Brewer Mk II 016, Mk III 178	50.80	4.36	100
Saturna Island	MSC	Brewer Mk II 012	48.77	-123.13	178
Ft. Peck	NEUBrew	Brewer Mk IV 147	48.31	-105.10	634
Davos	PMOD-WRC	Brewer Mk III 163	46.82	9.85	1590
Aosta	ARPA-VDA	Brewer Mk IV 066	45.74	7.36	570
Uni. Toronto	U. Toronto	Brewer Mk IV 083	43.66	-79.40	174
Kislovodsk	RAS-IAP	Brewer Mk II 043	43.73	42.66	2070
Sapporo	JMA	Brewer Mk III 169	43.06	141.33	17
Thessaloniki	AUTH	Brewer Mk III 086	40.63	22.97	60
Bondville	NEUBrew	Brewer Mk IV 144	40.05	-88.37	213
MRS Niwot Ridge	NEUBrew	Brewer Mk IV 146	40.03	-105.53	2923
Tsukuba	JMA	Brewer Mk III 173, 200	36.06	140.13	31
Raleigh	NEUBrew	Brewer Mk IV 140	35.73	-78.68	272
Houston	NEUBrew	Brewer Mk IV 154	29.72	-95.34	64
Naha	JMA	Brewer Mk III 175	26.21	127.69	28
Cape D'Aguilar	HKPU	Brewer Mk IV 115	22.21	114.26	60
Palmer	NSF, NOAA	SUV-100	-64.77	-64.05	21
Syowa	JMA	Brewer Mk III 168, 209	-69.01	39.58	22
Utsteinen	RMIB	Brewer Mk III 100	-71.95	23.35	1350
McMurdo	NSF, NOAA	SUV-100	-77.83	166.67	183

Chapter 3

Validation results

3.1 Comparison with ground based measurements

The GOME-2 (sat) OUV RECO erythemally weighted [RD2] daily doses and daily maximum erythemal dose rates were compared with ground based measurements (gr). The percentage relative differences $100\% \cdot (\text{sat} - \text{gr}) / \text{gr}$, their means, root-mean-square errors (rRMSE), medians and 25th and 75th percentiles are listed in Tables 3.1 – 3.4. The histograms for percentage relative difference distributions binned with 10% interval were plotted for all stations. Four sites representing northern high latitudes, northern middle latitudes, low latitudes and southern high latitudes are shown in Figures 3.1 – 3.4, and the other stations are plotted in Appendix A ordered by latitudes from North to South. In the scatter plots the data sets were divided into four seasons (December–February, blue), (March–May, green), (June–August, red) and (September–December, black).

For daily doses, the median of relative differences from ground based measurements was less or equal to 10% at 23 sites. The average of the medians of all stations, excluding McMurdo and Syowa, was -1.20%. For daily maximum dose rates, the relative difference was less or equal to 10% at 18 sites. The average of the medians was -5.4%, when excluding McMurdo and Syowa from the analysis. At Kislodovsk, Syowa and McMurdo, the median of the relative differences was equal or larger than 20% for both the erythemally weighted daily dose and the maximum dose rates. At Kislodovsk the reason for large differences between satellite and ground based was the inhomogeneous surface of the site. The stations of Syowa and McMurdo are located at the coast of the Antarctic, where high reflectivity from snow and ice together with changing sea ice conditions increase uncertainties in satellite retrievals. There still exist challenges in discrimination of snow and clouds for extreme conditions, like in spring at the high latitude site of Barrow.

Small underestimation of maximum dose rates is a common feature for most of the stations. This is most probably due to changing cloud cover conditions: Interpolation of satellite over pass cloud optical depth is used to retrieve daily maximum dose rate. This cloud estimation can differ from real cloudiness. This is the case when there are rapidly moving clouds and the sun appears just at the moment of a ground based measurements, even if half an hour before or after, at the time of the satellite over pass, the sky was

covered by clouds.

Even if the aerosols are better taken into account in the OUV RECO than in the OUV OPER v1, there still exist challenges during specific conditions. For example at Thessaloniki in spring, the largest differences between satellite retrievals and ground based measurements could be explained with rapidly changing cloudiness and variability in aerosols due to Sahara dust and biomass burning.

The OUV RECO products include error estimates following [AD3]. The statistics of Tables 3.1 – 3.4 were calculated for two different data sets: The first including all data. The second including only data which error estimate was less than 100% of the measurement. Large error estimates were due to large uncertainties in input parameters. This is the case e.g. over highly reflecting snow or ice covered regions at high latitudes [AD3]. An example of the use of the error estimates is shown for Barrow in Figure 3.5, from which can be seen that the median relative difference for daily maximum UV dose rates was reduced from -15% to -5% when the error estimate was used to filter the data. The rRMSE was reduced from 41% to 26%.

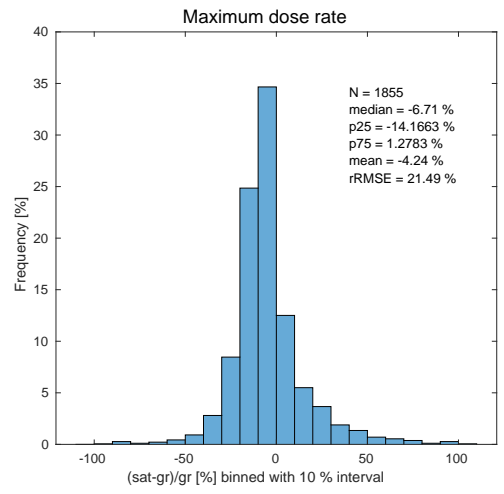
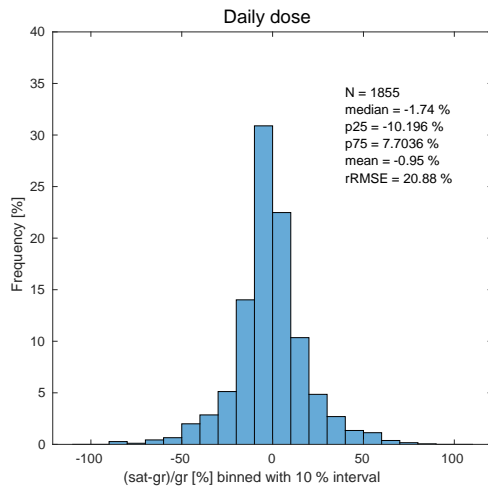
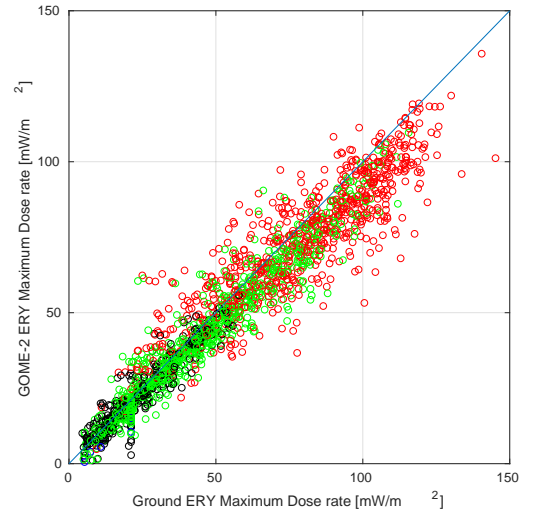
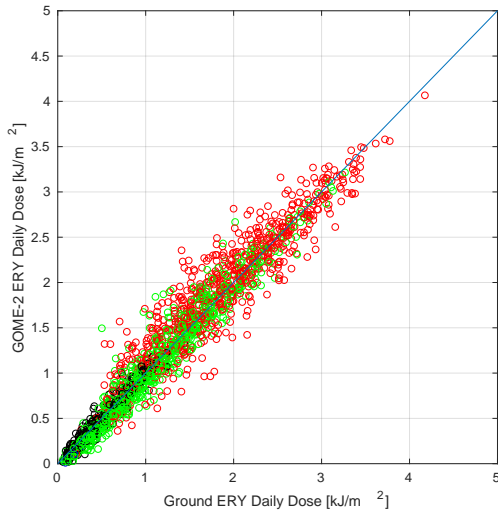


Figure 3.1: Sodankylä

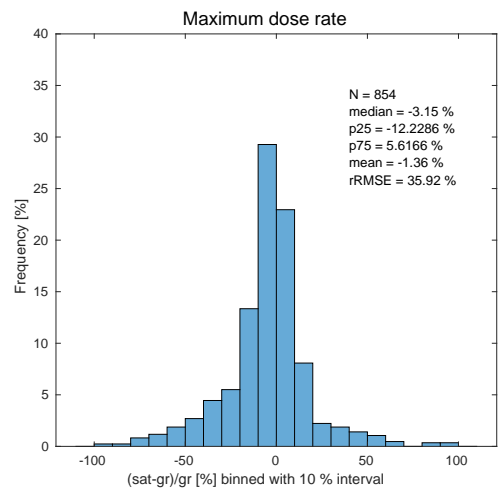
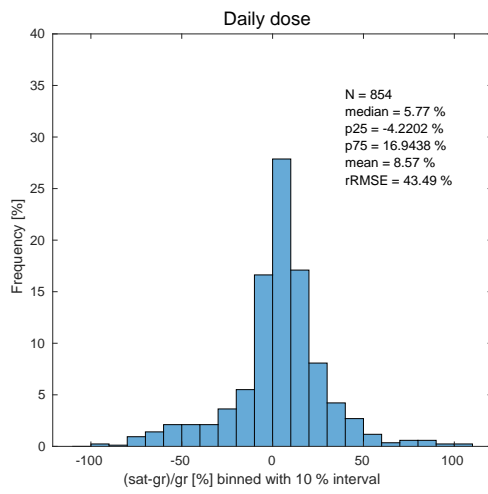
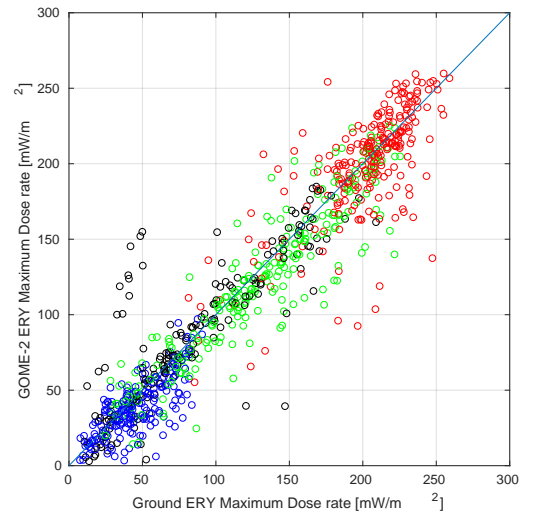
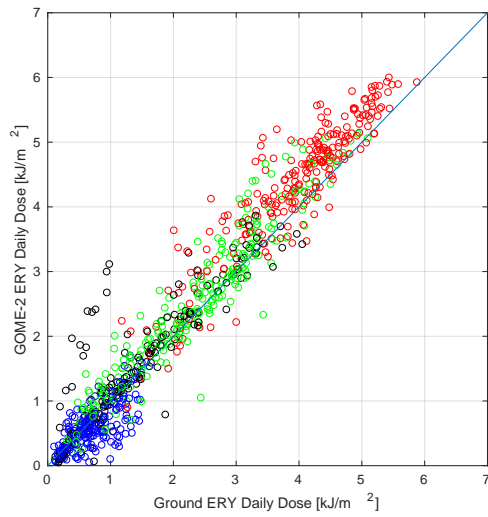


Figure 3.2: Bondville

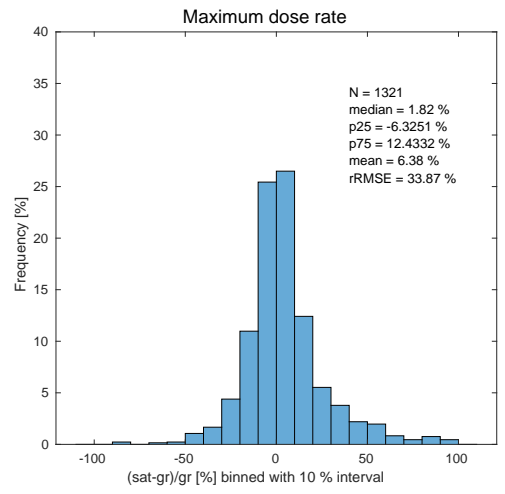
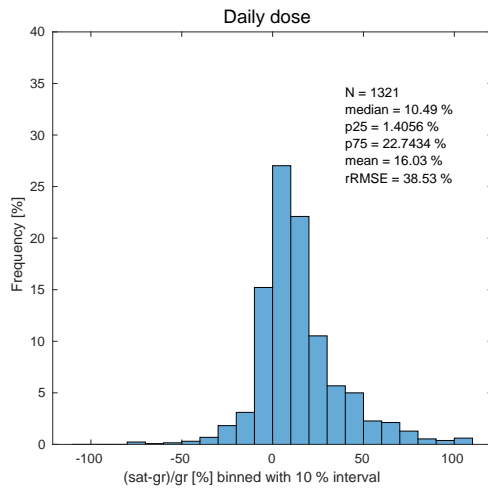
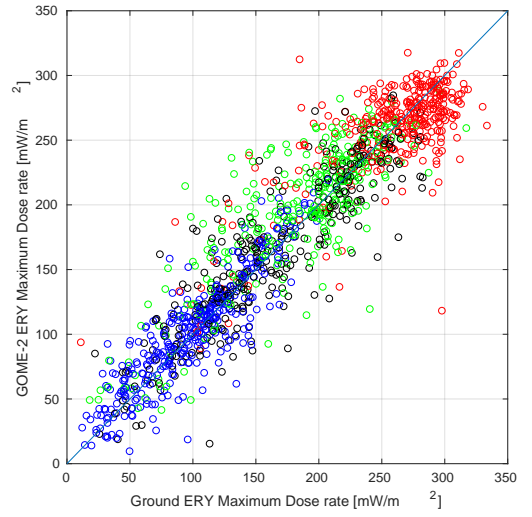
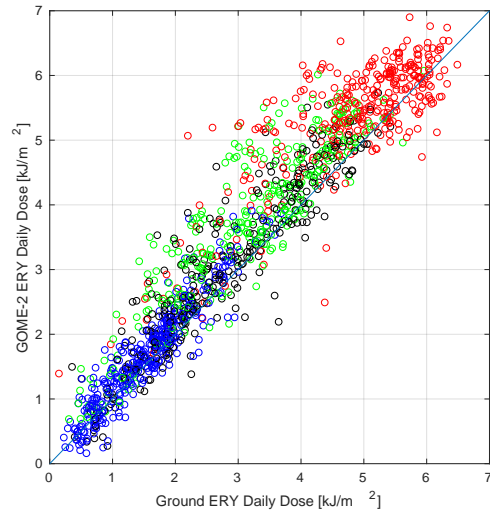


Figure 3.3: Naha

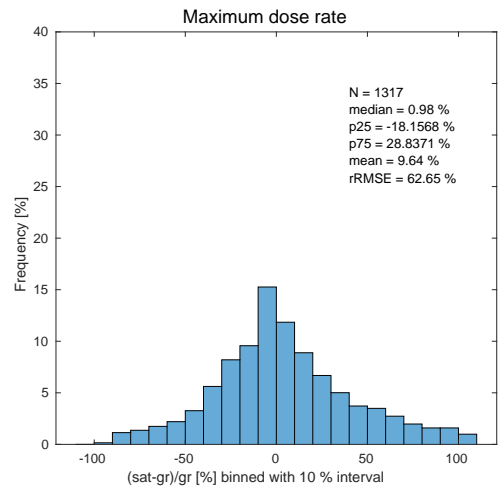
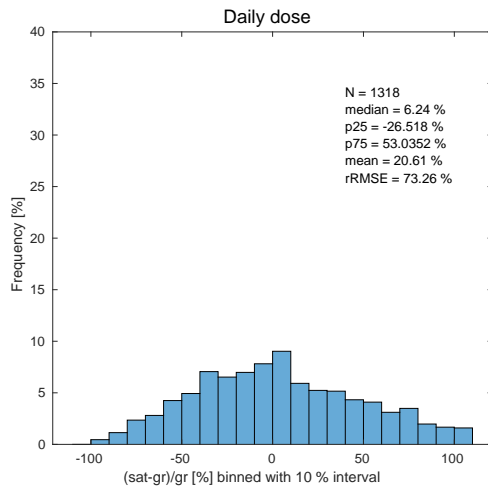
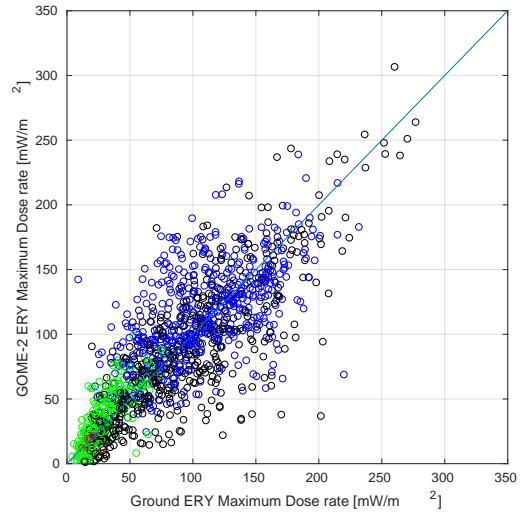
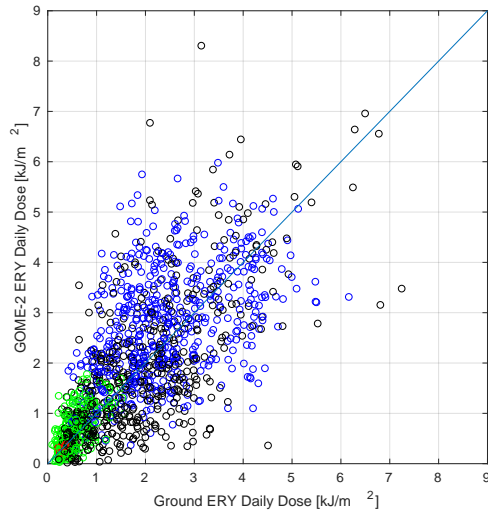


Figure 3.4: Palmer

Table 3.1: OUV RECO (sat) Erythemally weighted daily doses [RD2] compared to ground based measurements (gr). The percentage relative differences $100\% \cdot (\text{sat-gr})/\text{gr}$, their means (mean), root-mean-square errors (rRMSE), medians (median) and 25th (p25) and 75th (p75) percentiles were calculated. N is the number of measurement days included in the study.

Station	N	median [%]	p25 [%]	p75 [%]	mean [%]	rRMSE [%]
Summit (all data)	1082	-1.16	-5.50	3.31	-2.39	13.48
Summit ($1 \sigma < 100\%$)	1067	-1.11	-5.33	3.35	-1.06	7.22
Barrow (all data)	1029	-15.48	-62.59	12.28	-17.23	59.61
Barrow ($1 \sigma < 100\%$)	532	7.9	-6.94	28.21	16.99	55.69
Sodankylä (all data)	1855	-1.74	-10.20	7.70	-0.95	20.88
Sodankylä ($1 \sigma < 100\%$)	1158	0.10	-5.63	7.99	2.7	14.15
Jokioinen (all data)	1994	-0.85	-10.47	9.09	-0.44	23.55
Jokioinen ($1 \sigma < 100\%$)	1382	1.22	-4.23	11.07	5.27	18.65
Helsinki (all data)	307	4.75	-2.7	17.54	10.11	29.46
Helsinki ($1 \sigma < 100\%$)	219	5.3	-0.63	16.66	10.39	22.89
Churchill (all data)	978	-8.01	-29.36	3.73	-9.98	31.94
Churchill ($1 \sigma < 100\%$)	547	-1.19	-7.91	10.06	3.87	22.72
Tomsk (all data)	718	-4.01	-17.04	6.89	-3.02	23.75
Tomsk ($1 \sigma < 100\%$)	543	-1.5	-11.63	8.67	1.14	21.44
Obninsk (all data)	759	-1.38	-15.30	7.79	-2.79	24.83
Obninsk ($1 \sigma < 100\%$)	551	1.29	-8.10	10.11	2.49	20.96
Edmonton (all data)	549	-5.51	-14.18	1.91	-5.89	21.58
Edmonton ($1 \sigma < 100\%$)	432	-3.46	-8.90	3.17	-1.58	15.94
Goose Bay (all data)	1287	-3.78	-15.63	6.72	-3.76	25.9
Goose Bay ($1 \sigma < 100\%$)	929	-1.16	-9.54	7.99	1.5	20.44
Uccle (all data)	1128	8.3	1.95	18.99	11.54	23.08
Uccle ($1 \sigma < 100\%$)	945	9.01	3.69	19.01	12.75	20.69
Saturna Island (all data)	1487	0.79	-6.71	14.91	11.25	49.15
Saturna Island ($1 \sigma < 100\%$)	1135	1.41	-4.23	13.56	10.53	38.73
Ft. Peck (all data)	1413	2.72	-11.28	10.83	-2.6	31.9
Ft. Peck ($1 \sigma < 100\%$)	988	5.83	-0.07	13.09	8.97	21.96

Table 3.2: Same as in Table 3.1.

Station	N	median [%]	p25 [%]	p75 [%]	mean [%]	rRMSE [%]
Davos (all data)	1482	-12.72	-44.26	1.27	-15.95	52.8
Davos ($1 \sigma < 100\%$)	827	-1.22	-9.63	10.329	6.8	53.26
Aosta (all data)	1097	-12.24	-37.23	7.21	-5.41	104.23
Aosta ($1 \sigma < 100\%$)	610	3.62	-9.18	15.62	21.45	132.39
Toronto (all data)	179	-0.07	-6.43	9.60	1.77	21.28
Toronto ($1 \sigma < 100\%$)	135	1.42	-4.32	9.23	3.92	14.75
Kislovodsk (all data)	1263	-34.83	-56.86	-12.74	-32.61	46.03
Kislovodsk ($1 \sigma < 100\%$)	345	-9.13	-16.58	2.35	-2.64	25.18
Sapporo (all data)	1819	-4.34	-24.74	10.40	-5.93	34.56
Sapporo ($1 \sigma < 100\%$)	1107	3.09	-6.53	15.17	7.47	26.63
Thessaloniki (all data)	1521	6.71	-8.93	21.22	19.74	85.4
Thessaloniki ($1 \sigma < 100\%$)	1231	10.09	-0.39	24.86	29.79	86.72
Bondville (all data)	854	5.77	-4.22	16.94	8.57	43.49
Bondville ($1 \sigma < 100\%$)	666	7.02	-0.56	17.02	13.38	38.98
Niwot Ridge (all data)	1517	-7.73	-24.04	8.00	19.27	207.9
Niwot Ridge ($1 \sigma < 100\%$)	949	-4.23	-12.62	11.41	23.47	187.97
Tsukuba (all data)	1609	9.64	3.45	19.09	12.04	25.6
Tsukuba ($1 \sigma < 100\%$)	1381	10.24	5.08	18.93	13.5	21.29
Raleigh (all data)	1363	4.38	-1.84	10.27	4.21	18.66
Raleigh ($1 \sigma < 100\%$)	1148	5.08	0.60	10.51	6.88	14.68
Houston (all data)	267	19.13	7.19	28.24	17.07	27.36
Houston ($1 \sigma < 100\%$)	223	21.49	10.23	29.49	21.84	26.96
Naha (all data)	1321	10.49	1.41	22.74	16.03	38.53
Naha ($1 \sigma < 100\%$)	1078	10.96	3.25	21.71	16.72	29.39
Cape D'Aguilar (all data)	257	1.9	-5.91	23.16	26.96	88.82
Cape D'Aguilar ($1 \sigma < 100\%$)	230	1.58	-5.51	20.72	27.33	91.41
Palmer (all data)	1318	6.24	-26.52	53.04	20.61	73.26
Palmer ($1 \sigma < 100\%$)	476	23.01	-2.50	71.51	44.05	84.07
Syowa (all data)	951	-49.39	-65.66	-30.80	-48.16	53.17
Syowa ($1 \sigma < 100\%$)	-	-	-	-	-	-
Utsteinen (all data)	52	-0.43	-19.22	1.96	-15.22	33.03
Utsteinen ($1 \sigma < 100\%$)	-	-	-	-	-	-
McMurdo (all data)	757	-57.00	-68.62	-44.87	-54.58	58.2
McMurdo ($1 \sigma < 100\%$)	-	-	-	-	-	-

Table 3.3: OUV RECO (sat) daily maximum erythemally weighted [RD2] dose rates compared to ground based measurements (gr). The percentage relative differences $100\% \cdot (\text{sat-gr})/\text{gr}$, their means (mean), root-mean-square errors (rRMSE), medians (median) and 25th (p25) and 75th (p75) percentiles were calculated. N is the number of measurement days included in the study.

Station	N	median [%]	p25 [%]	p75 [%]	mean [%]	rRMSE [%]
Summit (all data)	1075	-2.72	-6.48	-0.14	-2.53	36.89
Summit ($1 \sigma < 100\%$)	1060	-2.66	-6.17	-0.11	-1.22	35.36
Barrow (all data)	1029	-15.25	-48.89	0.44	-22.11	41.09
Barrow ($1 \sigma < 100\%$)	690	-4.55	-16.50	4.96	-4.84	26.54
Sodankylä (all data)	1855	-6.71	-14.17	1.28	-4.24	21.49
Sodankylä ($1 \sigma < 100\%$)	1707	-6.45	-13.59	0.73	-3.68	19.39
Jokioinen (all data)	1994	-5.1	-13.63	2.90	-3.23	23.55
Jokioinen ($1 \sigma < 100\%$)	1808	-4.78	-12.38	2.82	-1.91	20.28
Helsinki (all data)	307	0.21	-8.5	9.19	6.25	33.97
Helsinki ($1 \sigma < 100\%$)	285	0.05	-8.16	8.00	5.42	31.89
Churchill (all data)	978	-11.92	-25.07	-2.36	-11.74	27.83
Churchill ($1 \sigma < 100\%$)	716	-9.00	-17.91	-0.61	-6.8	23.19
Tomsk (all data)	718	-11.43	-22.47	-2.06	-10.55	23.79
Tomsk ($1 \sigma < 100\%$)	664	-11.04	-20.894	-1.92	-9.74	22.33
Obninsk (all data)	759	-10.23	-23.38	-0.71	-11.24	26.43
Obninsk ($1 \sigma < 100\%$)	677	-9.66	-20.73	-0.28	-8.44	22.93
Edmonton (all data)	549	-10.83	-20.21	-4.79	-11.85	21.96
Edmonton ($1 \sigma < 100\%$)	523	-10.44	-18.06	-4.53	-10.63	20.47
Goose Bay (all data)	1287	-10.52	-22.10	-2.26	-11.29	25.94
Goose Bay ($1 \sigma < 100\%$)	1117	-9.52	-19.47	-1.51	-8.84	21.4
Uccle (all data)	1128	-5.29	-17.89	2.67	-7.47	20.43
Uccle ($1 \sigma < 100\%$)	1082	-4.61	-16.68	2.75	-6.96	18.74
Saturna Island (all data)	1487	-6.52	-16.57	1.40	0.16	49.13
Saturna Island ($1 \sigma < 100\%$)	1356	-5.88	-14.82	1.37	0.83	43.41
Ft. Peck (all data)	1413	-2.64	-14.71	4.06	-7.30	27.64
Ft. Peck ($1 \sigma < 100\%$)	1159	-0.95	-8.72	4.85	-0.86	18.97

Table 3.4: Same as in Table 3.3.

Station	N	median [%]	p25 [%]	p75 [%]	mean [%]	rRMSE [%]
Davos (all data)	1482	-19.21	-38.32	-6.72	-21.94	44.03
Davos ($1 \sigma < 100\%$)	1159	-13.85	-27.06	-4.51	-12.83	38.08
Aosta (all data)	1097	-9.85	-32.72	6.13	-7.63	85.12
Aosta ($1 \sigma < 100\%$)	879	-3.29	-21.35	8.73	3.00	89.79
Toronto (all data)	179	-4.52	-10.76	0.96	-3.87	21.4
Toronto ($1 \sigma < 100\%$)	161	-4.44	-9.31	0.86	-2.70	18.51
Kislovodsk (all data)	1263	-29.37	-51.37	-15.39	-32.81	42.11
Kislovodsk ($1 \sigma < 100\%$)	841	-21.02	-30.93	-10.98	-20.02	27.79
Sapporo (all data)	1819	-7.1	-25.67	5.46	-8.64	32.83
Sapporo ($1 \sigma < 100\%$)	1495	-3.44	-16.36	7.14	-1.9	26.27
Thessaloniki (all data)	1521	3.76	-11.19	14.71	13.11	74.99
Thessaloniki ($1 \sigma < 100\%$)	1390	4.94	-5.28	15.99	19.75	75.88
Bondville (all data)	854	-3.15	-12.23	5.62	-1.36	35.92
Bondville ($1 \sigma < 100\%$)	769	-2.33	-1.00	6.04	1.95	33.5
Niwot Ridge (all data)	1517	-15.4	-28.21	-6.73	6.13	199.92
Niwot Ridge ($1 \sigma < 100\%$)	1343	-13.96	-24.41	-6.21	10.02	207.95
Tsukuba (all data)	1609	6.27	-2.46	14.49	7.27	26.26
Tsukuba ($1 \sigma < 100\%$)	1517	6.72	-1.17	14.59	8.86	24.87
Raleigh (all data)	1363	-2.62	-13.01	3.65	-5.29	19.16
Raleigh ($1 \sigma < 100\%$)	1280	-1.88	-11.13	4.03	-3.33	15.69
Houston (all data)	267	5.27	-3.16	18.08	4.67	21.00
Houston ($1 \sigma < 100\%$)	254	6.37	-2.02	18.55	7.18	18.30
Naha (all data)	1321	1.82	-6.33	12.43	6.38	33.87
Naha ($1 \sigma < 100\%$)	1223	2.06	-5.43	12.37	6.93	32.41
Cape D'Aguilar (all data)	257	1.9	-5.91	23.16	26.96	88.82
Cape D'Aguilar ($1 \sigma < 100\%$)	250	-5.07	-12.78	7.05	11.99	67.87
Palmer (all data)	1317	0.98	-18.16	28.84	9.64	62.65
Palmer ($1 \sigma < 100\%$)	897	4.97	-9.99	31.18	16.48	66.22
Syowa (all data)	951	-28.59	-51.24	-14.15	-33.54	42.11
Syowa ($1 \sigma < 100\%$)	-	-	-	-	-	-
Utsteinen (all data)	52	-5.26	-21.67	-2.01	-17.09	30.14
Utsteinen ($1 \sigma < 100\%$)	-	-	-	-	-	-
McMurdo (all data)	744	-22.07	-42.93	-9.86	-27.43	36.67
McMurdo ($1 \sigma < 100\%$)	207	-8.9	-15.71	-1.87	-8.96	14.91

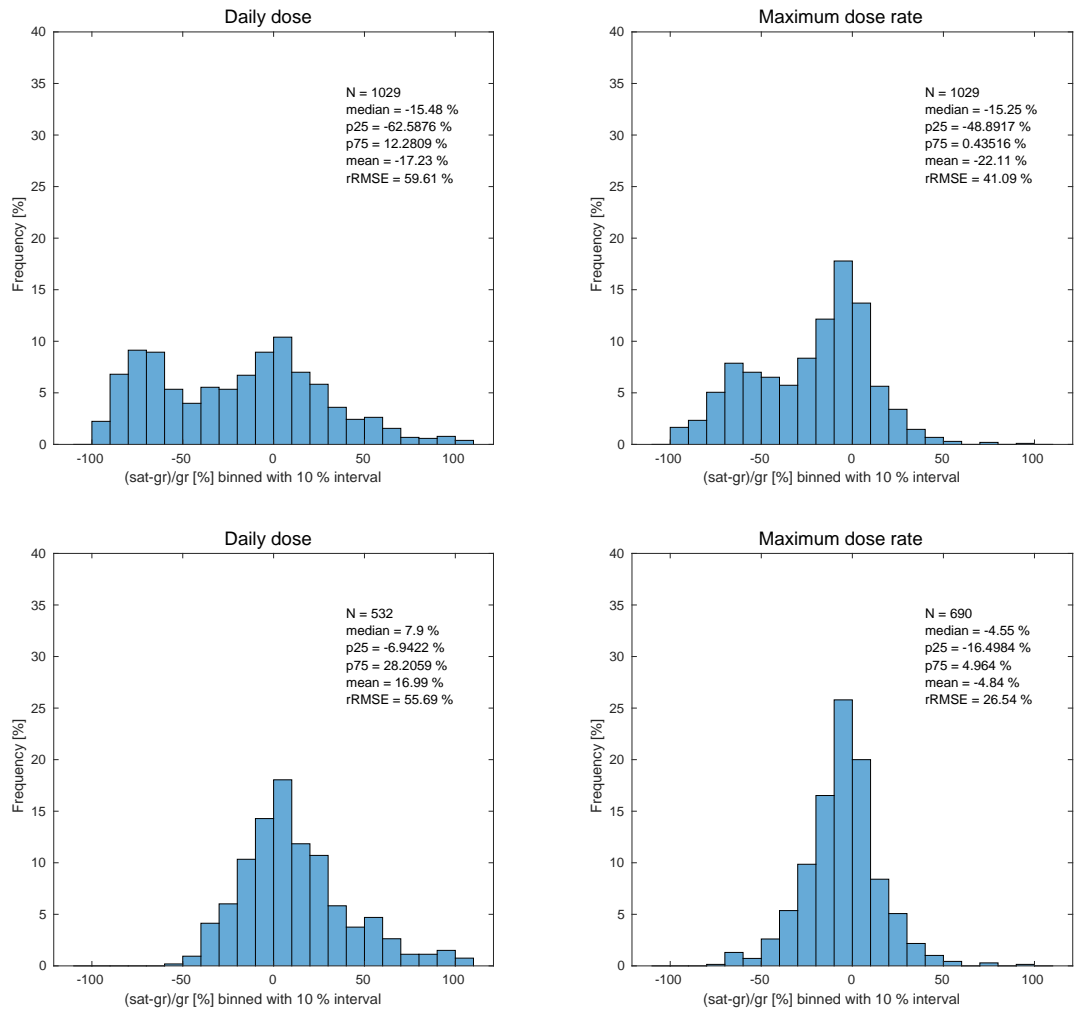


Figure 3.5: Statistics of the percentage relative differences $100\% \cdot (\text{sat-gr})/\text{gr}$ at Barrow calculated from two data sets: All data (top). Data which error estimate was less than 100% (bottom).

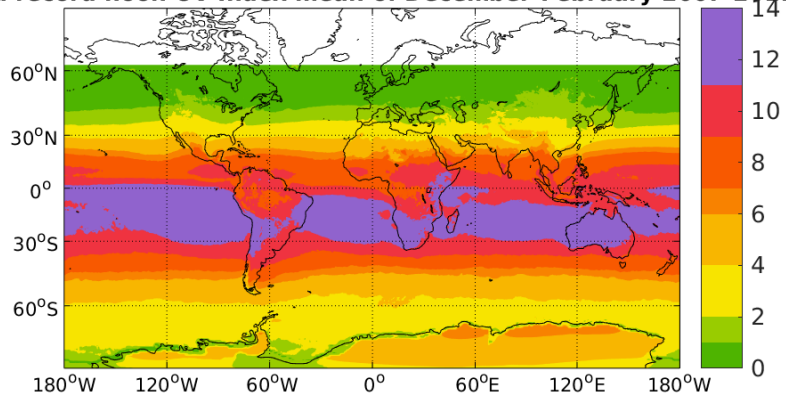
3.2 Differences between OUV OPER v1 and OUV RECO

The OUV RECO solar noon UV index was compared with the corresponding OUV OPER v1 product. The year was divided into four seasons: (December–February), (March–May), (June–August) and (September–December). The differences are shown in Figures 3.6–3.9. Low quality data [AD2,AD4] has been screened out from the data sets.

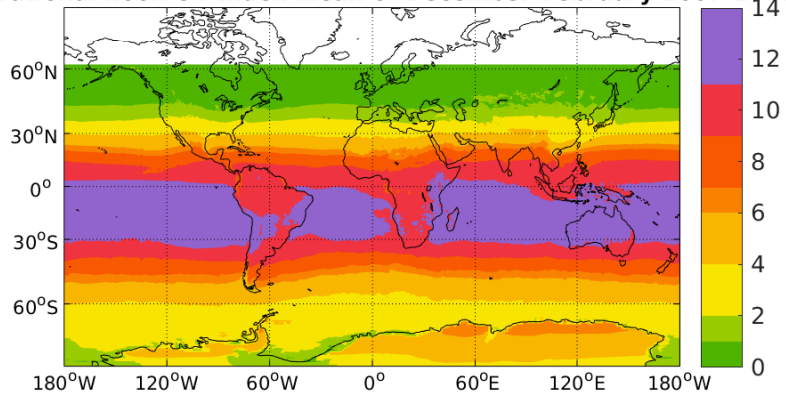
The OUV RECO erythemally weighted [RD2] daily dose was also compared with the corresponding OUV OPER v1 product. The corresponding median difference OUV RECO - OUV OPER v1 and relative difference $(\text{RECO} - \text{OPER}) / \text{OPER}$ as a function of latitude are also shown in Figures 3.10–3.13. Dashed lines show 16th and 84th percentiles of the distribution.

The largest differences were observed during transition periods (March-May and September-November), when surface albedo conditions differed from the climatology. This was the case at high latitudes during spring time. The OUV RECO showed lower values than OUV OPER v1. The median difference was around 30% and 60% in southern and northern hemisphere's high latitudes, correspondingly, for erythemally weighted daily doses.

Data record noon UV Index mean of December-February 2007-2017



Operational noon UV Index mean of December-February 2007-2017



Solar noon UV index, relative difference (data record - operational)/operational

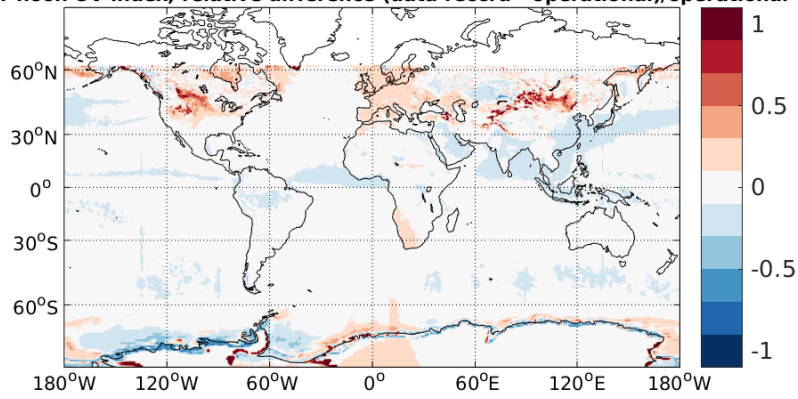


Figure 3.6: Mean solar noon UV index for December–February during 2007-2017. OUV RECO (top), OUV OPER v1 (second) and relative difference (bottom).

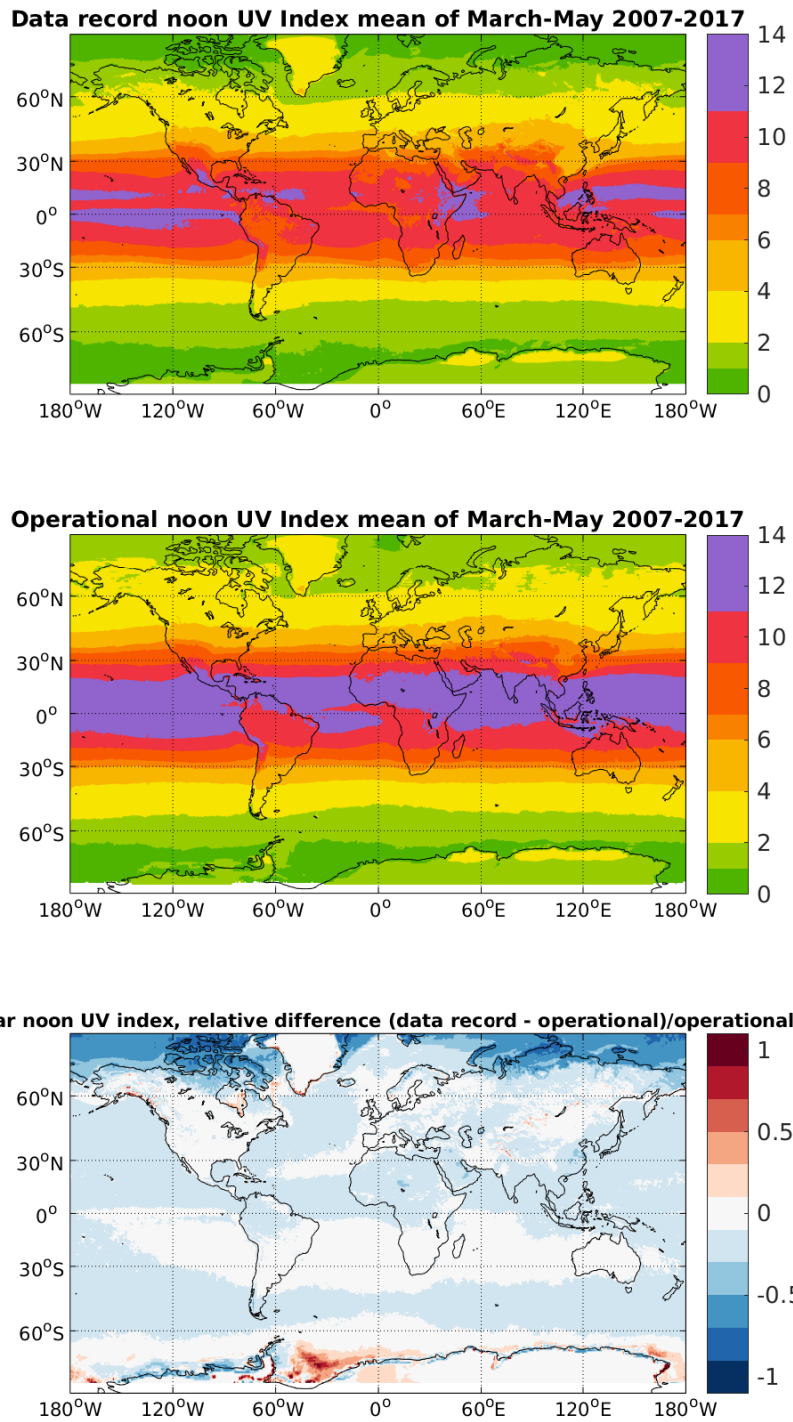
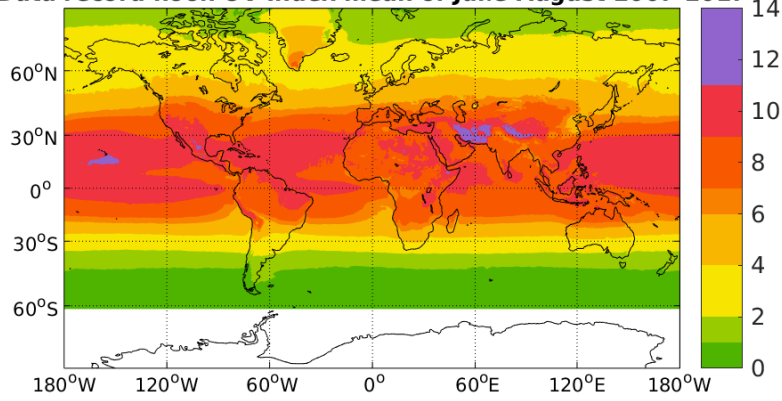
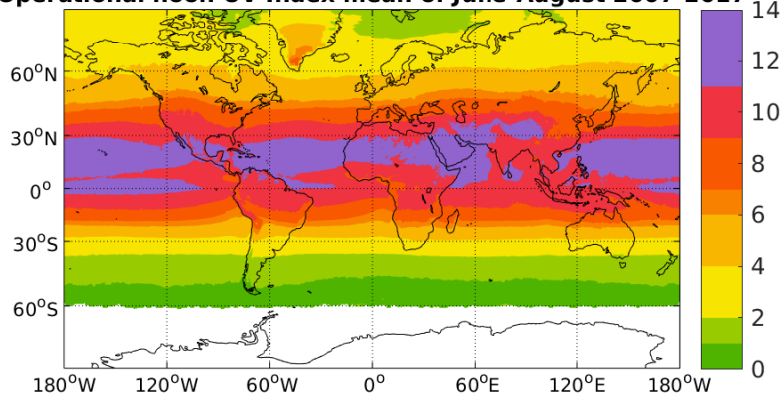


Figure 3.7: Mean solar noon UV index for March–May during 2007-2017. OUV RECO (top), OUV OPER v1 (second) and relative difference (bottom).

Data record noon UV Index mean of June-August 2007-2017



Operational noon UV Index mean of June-August 2007-2017



Solar noon UV index, relative difference (data record - operational)/operational

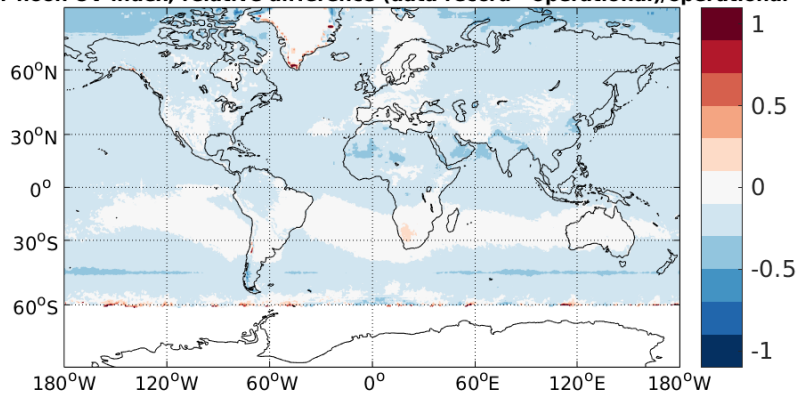
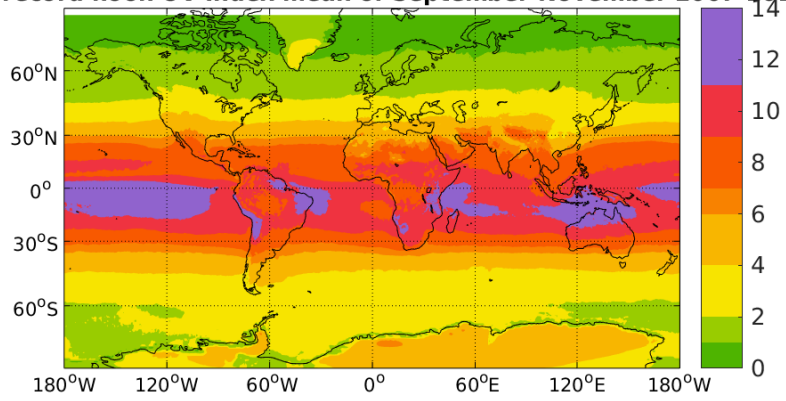
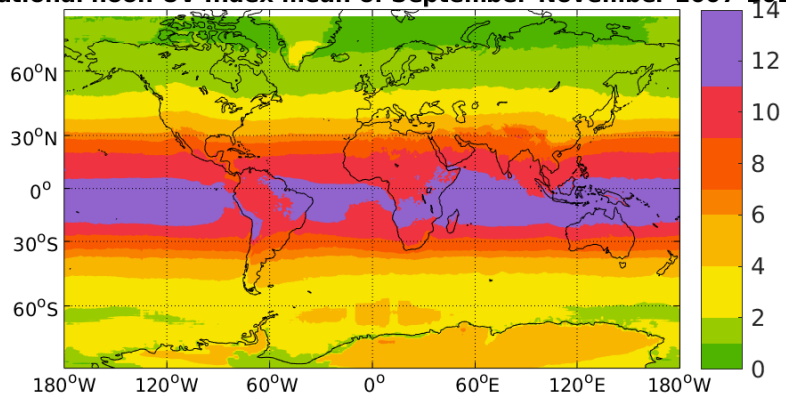


Figure 3.8: Mean solar noon UV index for June–August during 2007-2017. OUV RECO (top), OUV OPER v1 (second) and relative difference (bottom).

Data record noon UV Index mean of September–November 2007–2017



Operational noon UV Index mean of September–November 2007–2017



Solar noon UV index, relative difference (data record - operational)/operational

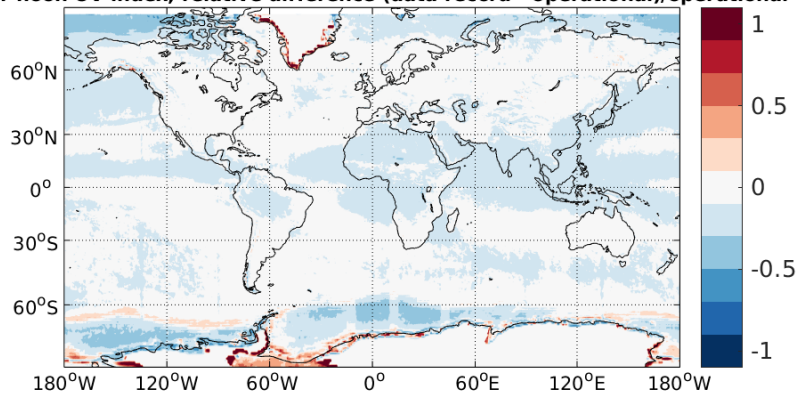


Figure 3.9: Mean solar noon UV index for September–November during 2007–2017. OUV RECO (top), OUV OPER v1 (second) and relative difference (bottom).

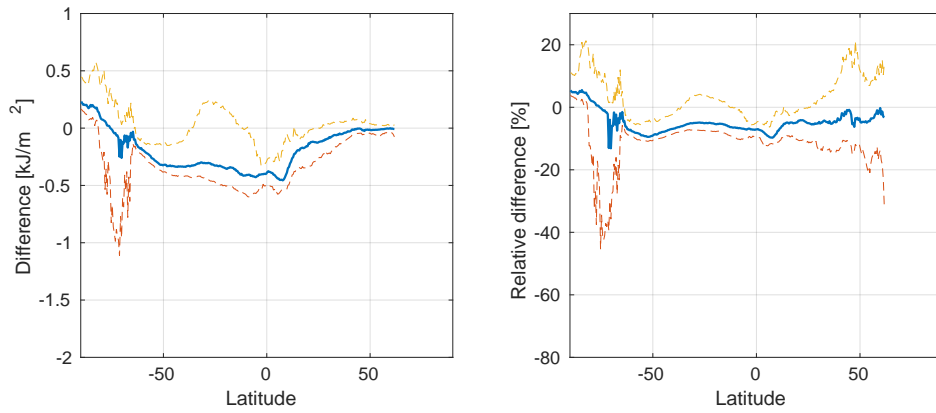


Figure 3.10: Median difference OUV RECO daily dose - OUV OPER v1 daily dose (left) and relative difference (RECO - OPER) / OPER (right) as a function of latitude for December–February during 2007-2017. Dashed lines show 16th and 84th percentiles of the distribution.

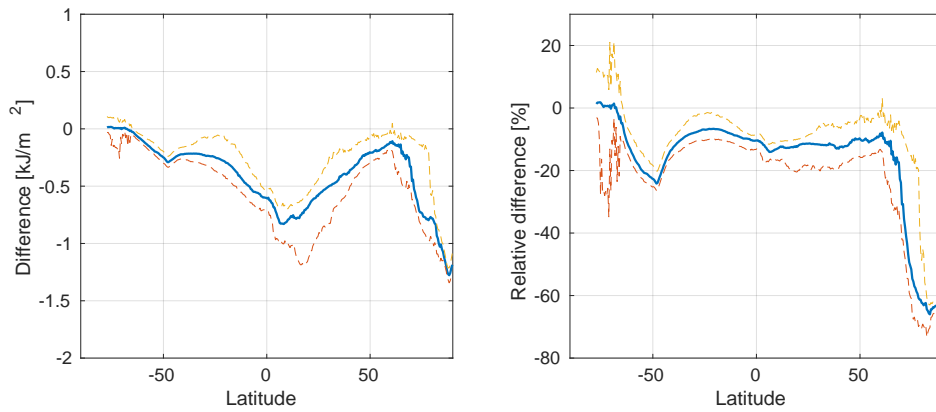


Figure 3.11: Median difference OUV RECO daily dose - OUV OPER v1 daily dose (left) and relative difference (RECO - OPER) / OPER (right) as a function of latitude for March–May during 2007-2017. Dashed lines show 16th and 84th percentiles of the distribution.

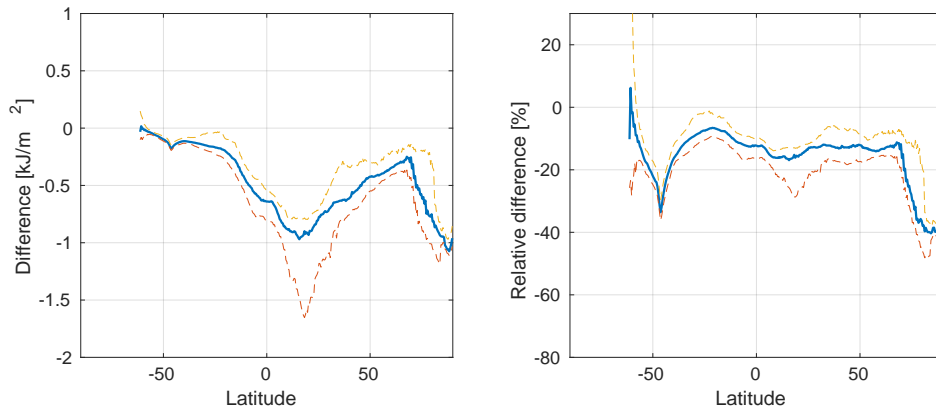


Figure 3.12: Median difference OUV RECO daily dose - OUV OPER v1 daily dose (left) and relative difference (RECO - OPER) / OPER (right) as a function of latitude for June–August during 2007-2017. Dashed lines show 16th and 84th percentiles of the distribution.

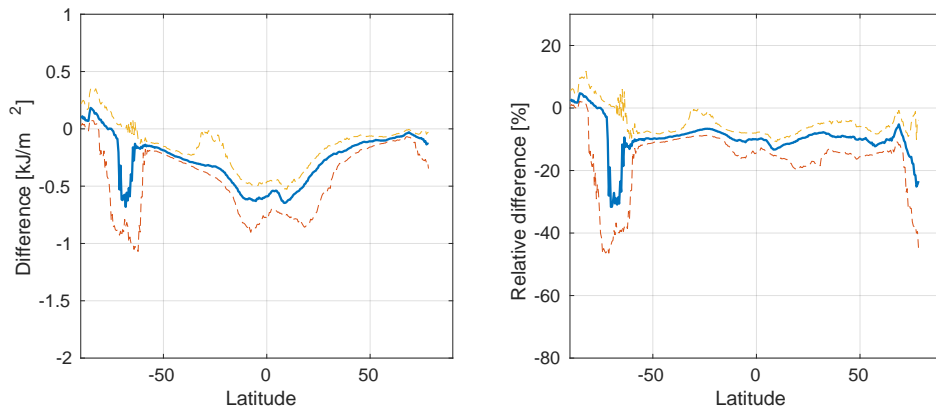


Figure 3.13: Median difference OUV RECO daily dose - OUV OPER v1 daily dose (left) and relative difference (RECO - OPER) / OPER (right) as a function of latitude for September–November during 2007-2017. Dashed lines show 16th and 84th percentiles of the distribution.

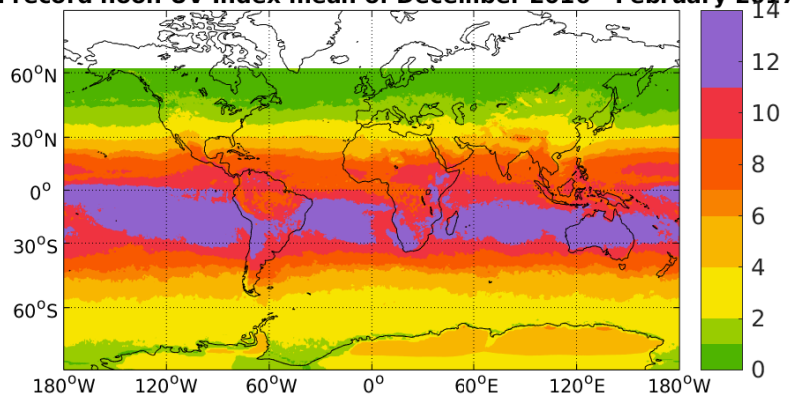
3.3 Differences between OUV OPER v2 and OUV RECO

The OUV OPER v2 solar noon UV index was compared with the corresponding OUV RECO product. The year was divided into four seasons: (December–February), (March–May), (June–August) and (September–December). The differences are shown in Figures 3.14–3.17. Low quality data [AD4] has been screened out from the data sets.

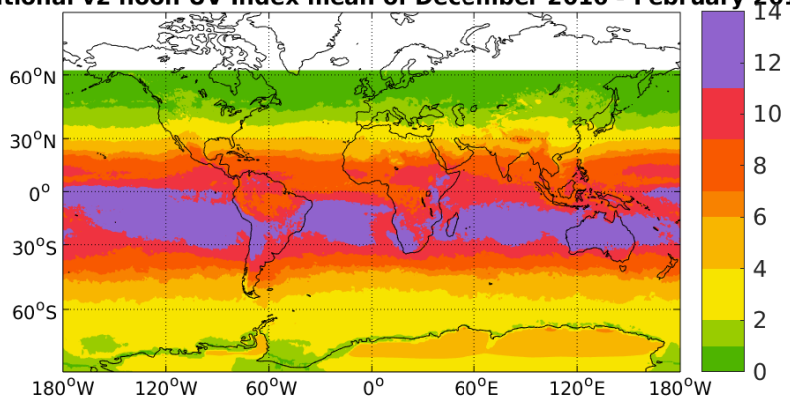
The OUV OPER v2 erythemally weighted [RD2] daily dose was also compared with the corresponding OUV RECO product. The corresponding median difference OUV OPER v2 - OUV RECO and relative difference $(\text{OPER v2} - \text{RECO}) / \text{RECO}$ as a function of latitude are also shown in Figures 3.18–3.21. Dashed lines show 16th and 84th percentiles of the distribution.

Differences were small, and mostly seen over inhomogeneous surfaces like southern and northern oceans, and mountainous areas, during transition periods. For December–February and June – August, the mean difference of erythemally weighted daily doses was less than $\pm 3\%$ for all latitudes, except for 63° – 68°S , where it was between 3 and 6% for the period December – February. For transition periods March – May and September – November, the mean difference was less than $\pm 3\%$ at all latitudes, except high latitudes. There, the mean difference was between -3 and -20% at latitudes higher than 64°N in March – May, and between 3 and 12 % at latitudes 61 – 67°S in September – November.

Data record noon UV Index mean of December 2016 - February 2017



Operational v2 noon UV Index mean of December 2016 - February 2017



Noon UV index, relative difference (operational v2 - data record)/data record

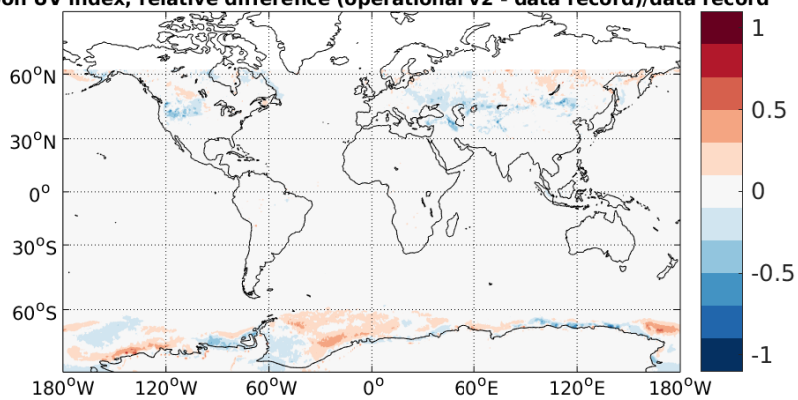


Figure 3.14: Mean solar noon UV index for December–February during 2007-2017. OUV RECO (top), OUV OPER v2 (second) and relative difference (bottom).

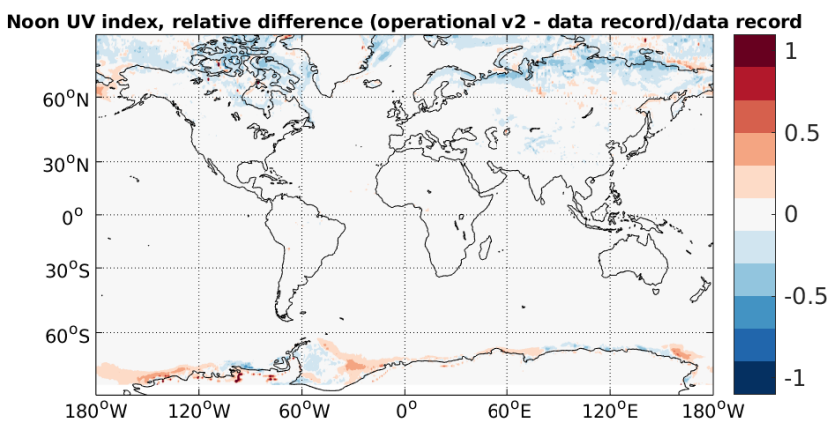
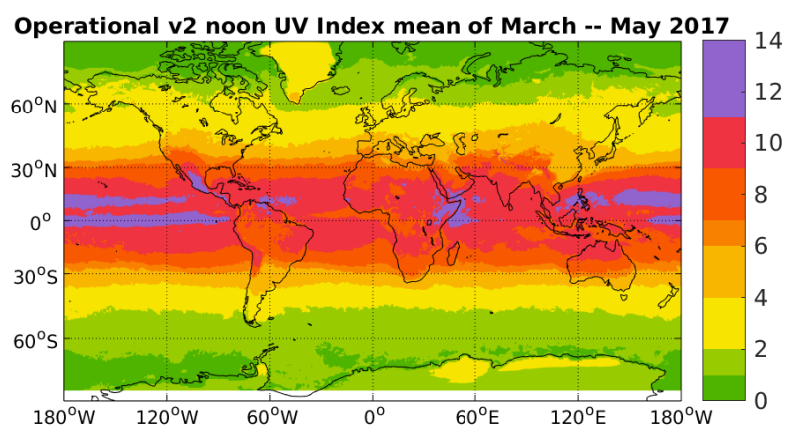
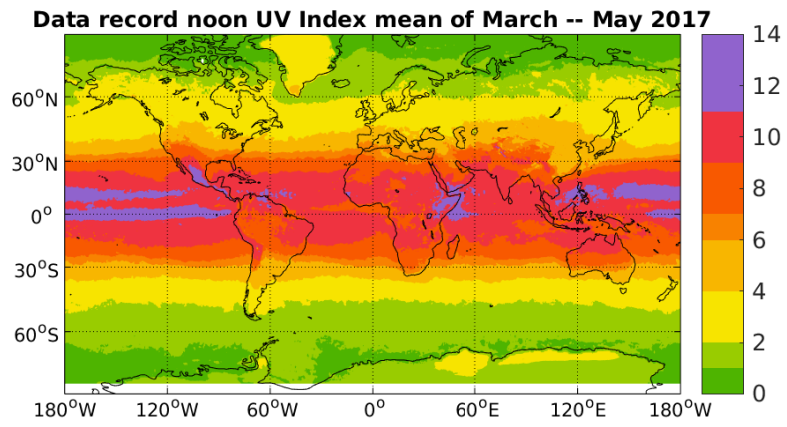


Figure 3.15: Mean solar noon UV index for March–May during 2007–2017. OUV RECO (top), OUV OPER v2 (second) and relative difference (bottom).

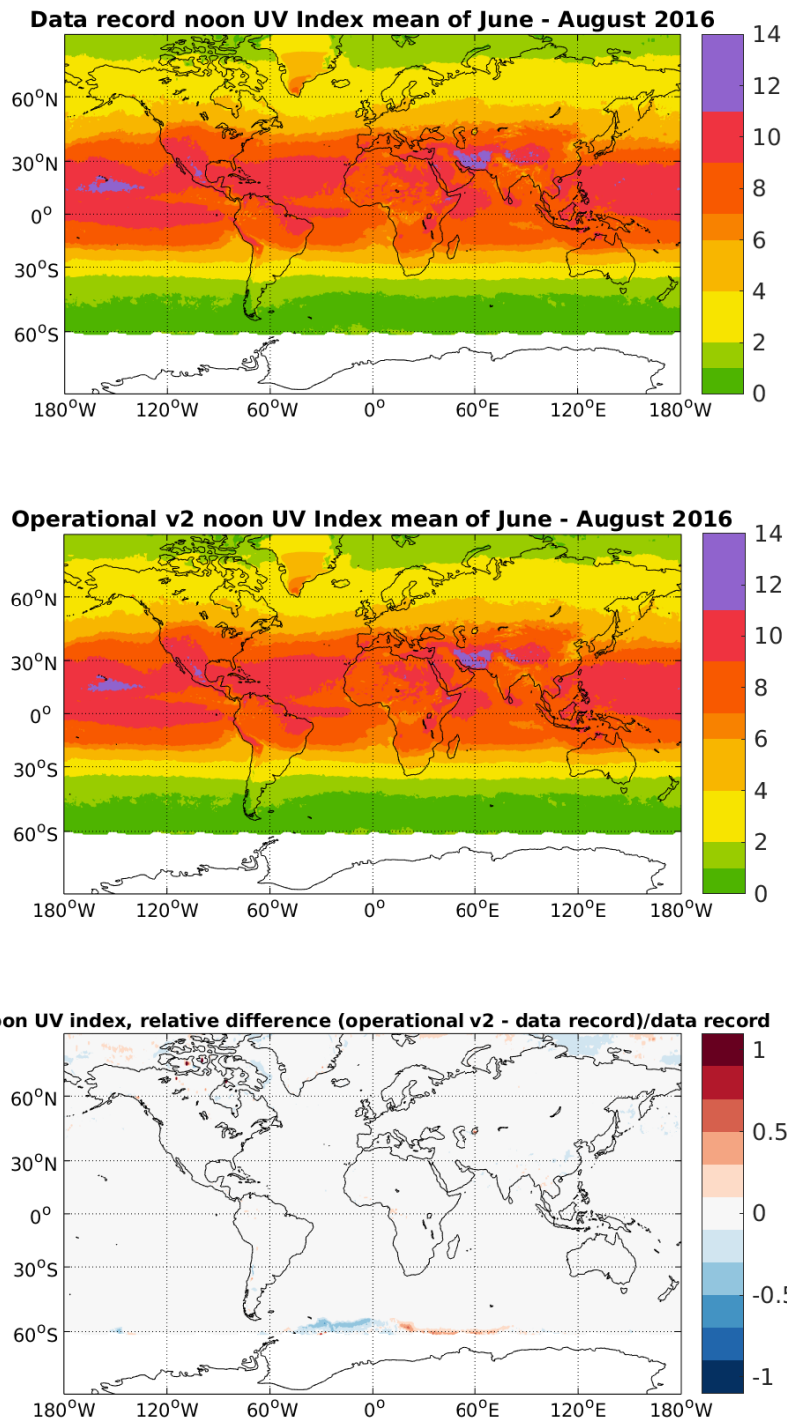
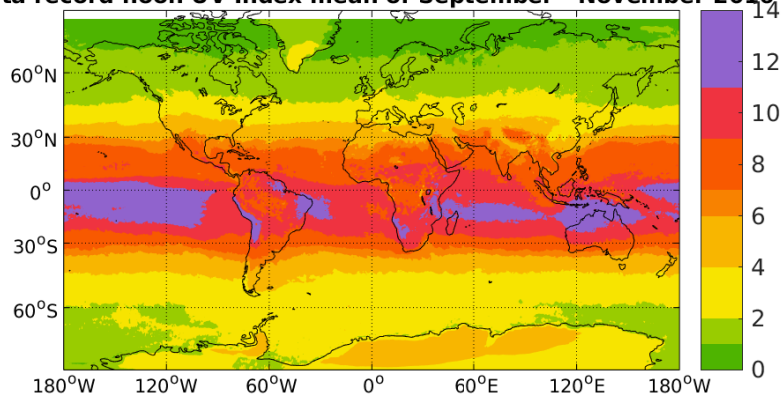
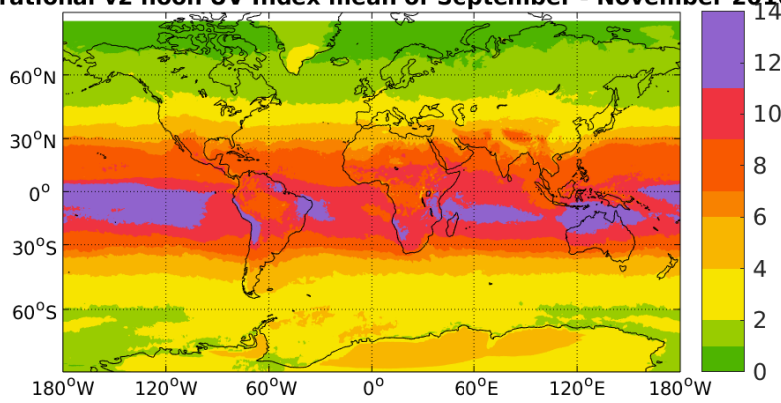


Figure 3.16: Mean solar noon UV index for June–August during 2007–2017. OUV RECO (top), OUV OPER v2 (second) and relative difference (bottom).

Data record noon UV Index mean of September - November 2016



Operational v2 noon UV Index mean of September - November 2016



Noon UV index, relative difference (operational v2 - data record)/data record

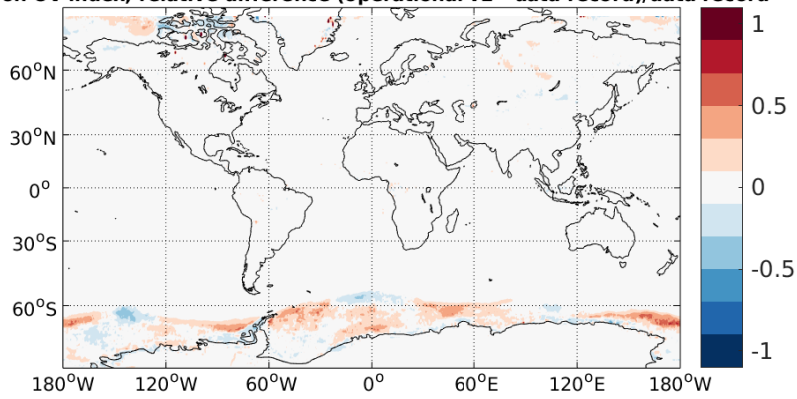


Figure 3.17: Mean solar noon UV index for September–November during 2007–2017. OUV RECO (top), OUV OPER v2 (second) and relative difference (bottom).

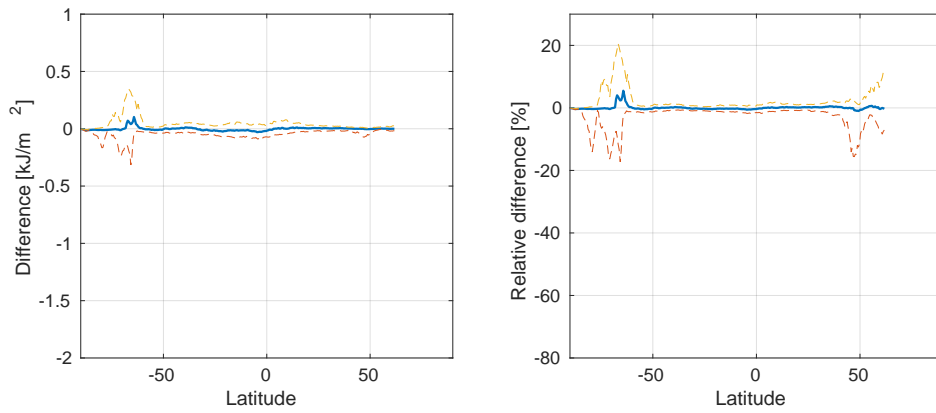


Figure 3.18: Median difference OUV OPER v2 daily dose - OUV RECO daily dose (left) and relative difference $(\text{OPER v2} - \text{RECO}) / \text{RECO}$ (right) as a function of latitude for December 2016 - February 2017. Dashed lines show 16th and 84th percentiles of the distribution.

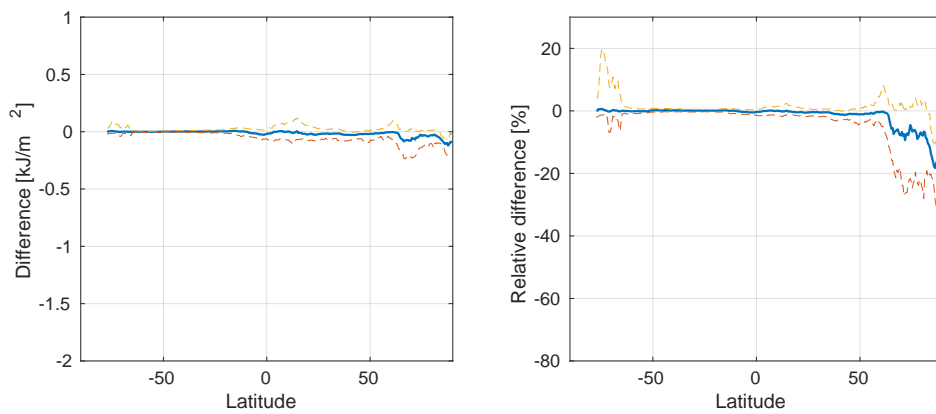


Figure 3.19: Median difference OUV OPER v2 daily dose - OUV RECO daily dose (left) and relative difference $(\text{OPER v2} - \text{RECO}) / \text{RECO}$ (right) as a function of latitude for March–May 2017. Dashed lines show 16th and 84th percentiles of the distribution.

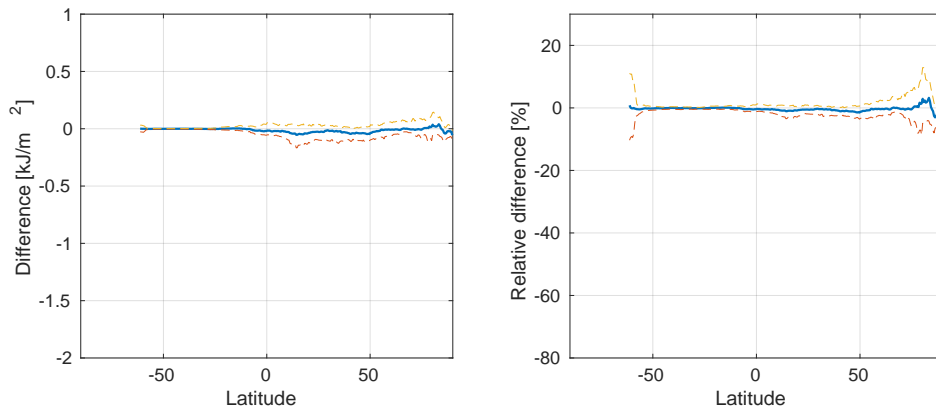


Figure 3.20: Median difference OUV OPER v2 daily dose - OUV RECO daily dose (left) and relative difference (OPER v2 - RECO) / RECO (right) as a function of latitude for June–August 2016. Dashed lines show 16th and 84th percentiles of the distribution.

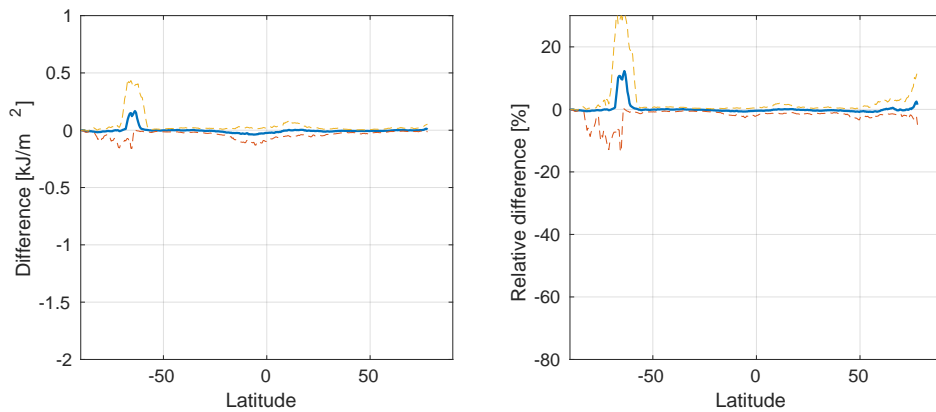


Figure 3.21: Median difference OUV OPER v2 daily dose - OUV RECO daily dose (left) and relative difference (OPER - RECO) / RECO (right) as a function of latitude for September–November 2016. Dashed lines show 16th and 84th percentiles of the distribution.

Chapter 4

Conclusions

The comparison of OUV RECO against ground based measurements showed that at most sites the difference was less or equal to 10%, even if challenges still remain at high latitudes under changing surface albedo conditions. For erythemally weighted daily doses, the average of the median differences was -1.20%, when excluding the Antarctic stations of Syowa and McMurdo. For erythemally weighted daily maximum dose rates, the average of the median differences was -5.4%. The error estimate of the UV product can be used to filter out data with highest uncertainties due to e.g., uncertainties in UV processor input parameters. For the validated products the following accuracy are specified in the service specification: Optimal 10%, Target 20% and Threshold 50%.

The comparison of OUV RECO against OUV OPER v1 showed that at most latitudes the difference was less than 20%, except at high latitudes, where the difference was higher during snow/ice melting periods.

The comparison of OUV OPER v2 against OUV RECO showed that differences were less than 3%, except over inhomogeneous surfaces like southern and northern high latitude oceans, and mountainous areas, during transition periods.

Chapter 5

Acknowledgments

The operators and data providers of ground based measurements are acknowledged. The SUV-100 spectroradiometer UV data from Summit and Barrow, as well as data from Palmer and McMurdo up to 2009, were provided by the NSF UV Monitoring Network (<http://uv.biospherical.com>), operated by Biospherical Instruments Inc. and funded by the U.S. National Science Foundation's Office of Polar Programs. Measurements at Palmer and McMurdo after 2009 were provided by NOAA's Antarctic UV Monitoring Network (<https://www.esrl.noaa.gov/gmd/grad/antuv/>). The data providers of NEUBrew network (<https://www.esrl.noaa.gov/gmd/grad/neubrew/index.jsp>) are acknowledged. Ground based UV data was downloaded from the WMO/GAW UV Radiation Monitoring Community, World Meteorological Organization-Global Atmosphere Watch Program (WMO-GAW)/World Ozone and Ultraviolet Radiation Data Centre (WOUDC) [Data]. Retrieved November 25, 2014, from <https://woudc.org>. A list of all contributors is available on the website doi:10.14287/10000002. We thank Anu Heikkilä from the Finnish Meteorological Institute for the Brewer data of Helsinki and Jokioinen, Henri Diemoz from the Agenzia Regionale per la Protezione dell'Ambiente Valle d'Aosta for the Brewer data of Aosta, and Alkiviadis Bais and Ilias Fountoulakis from the Aristotle University of Thessaloniki for the Brewer data of Thessaloniki.

APPENDIX A

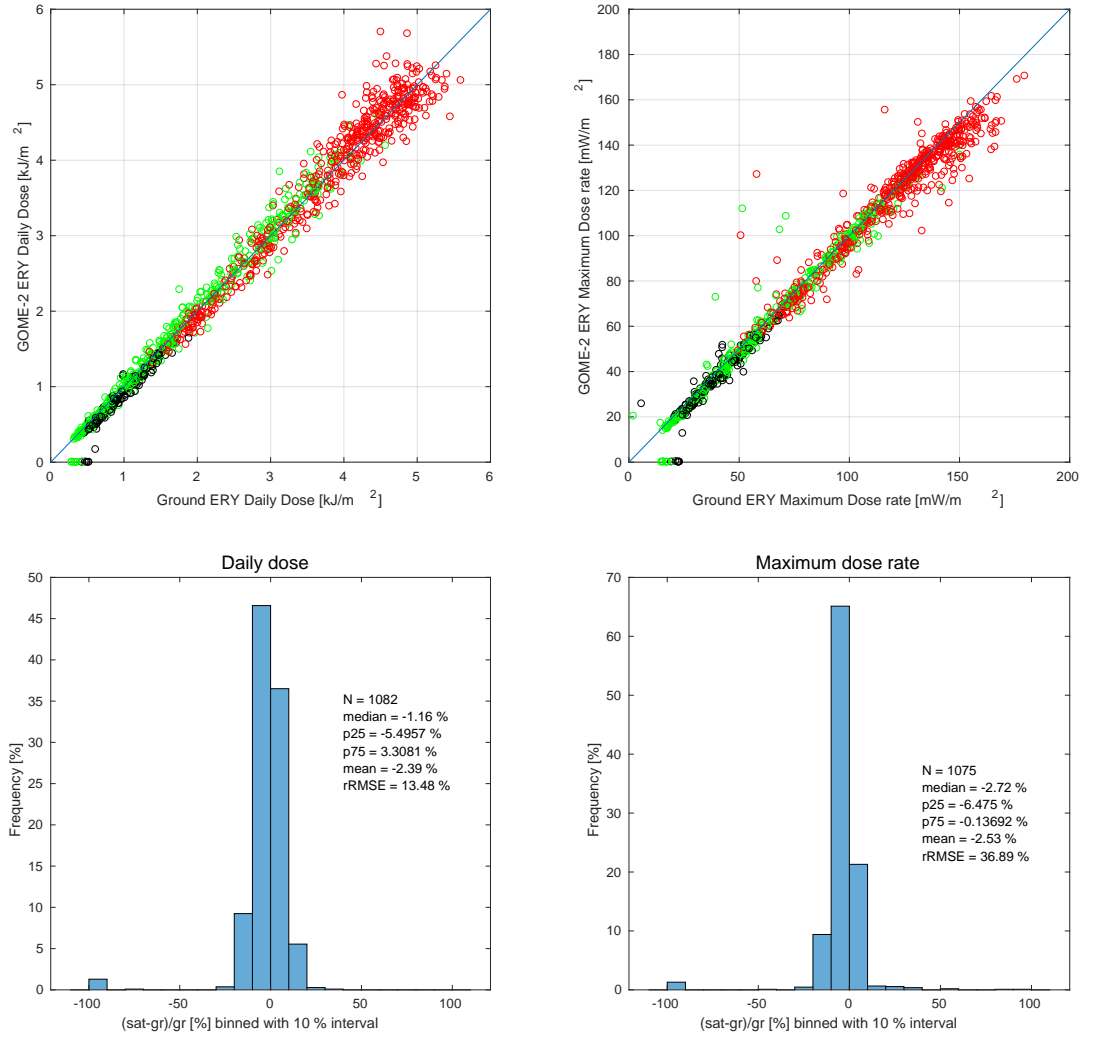


Figure 1: Summit

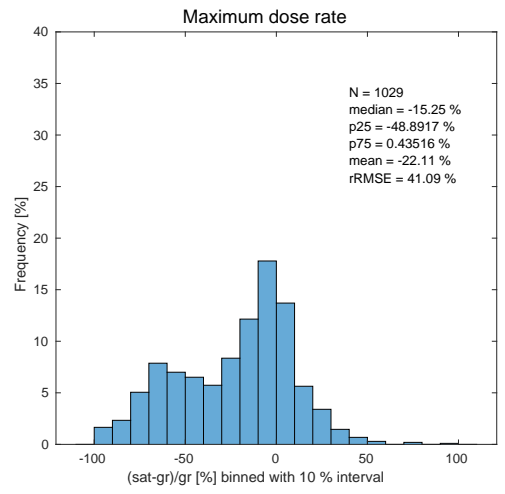
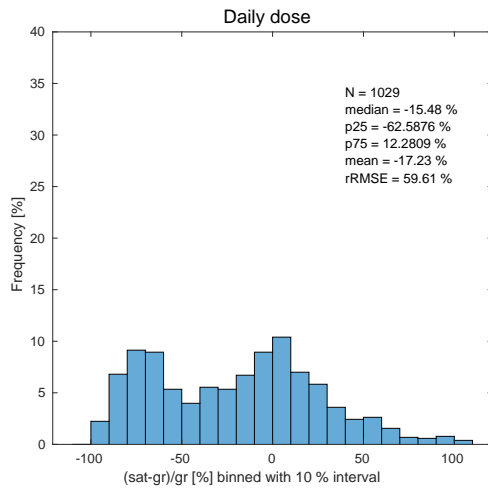
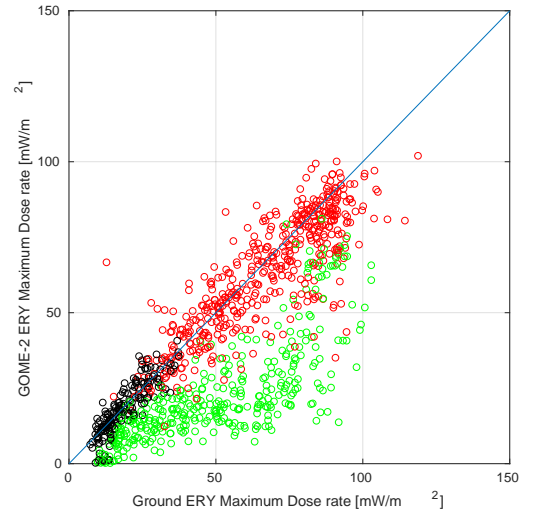
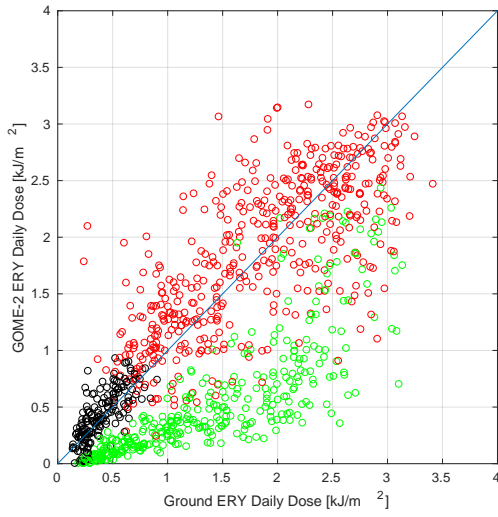


Figure 2: Barrow

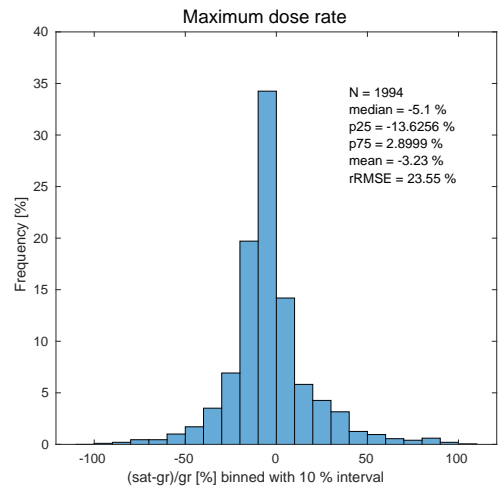
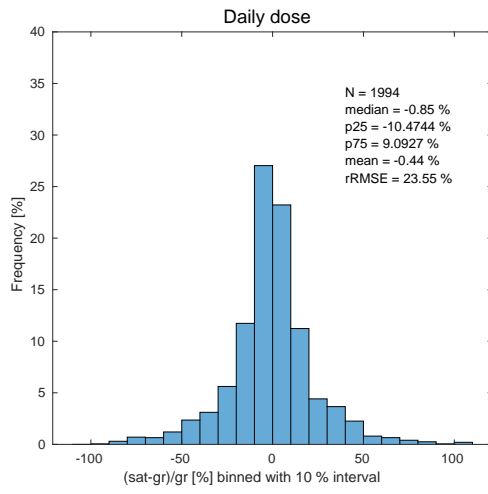
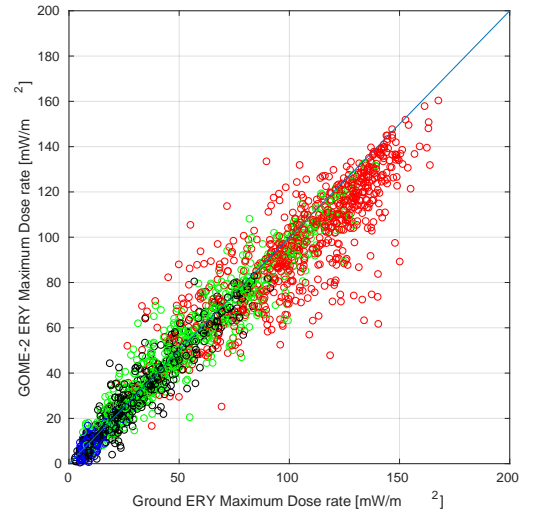
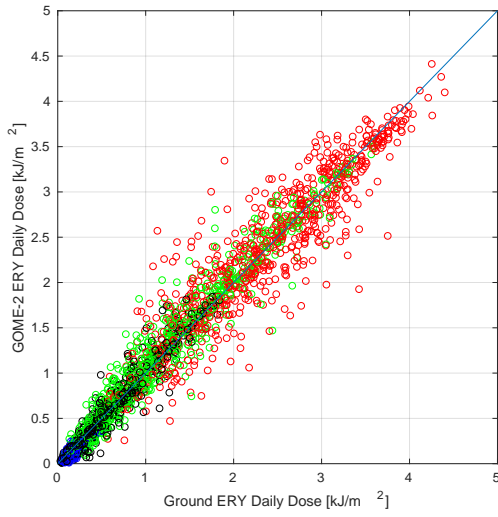


Figure 3: Jokioinen

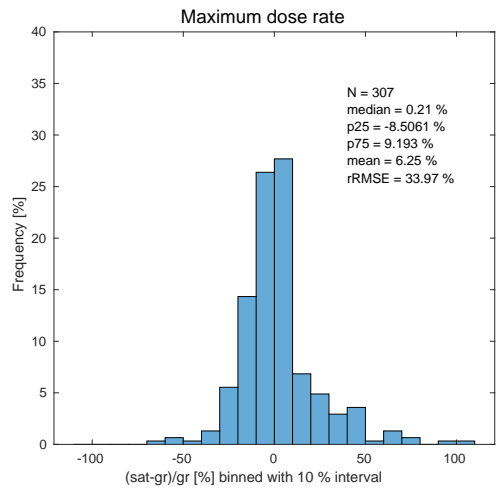
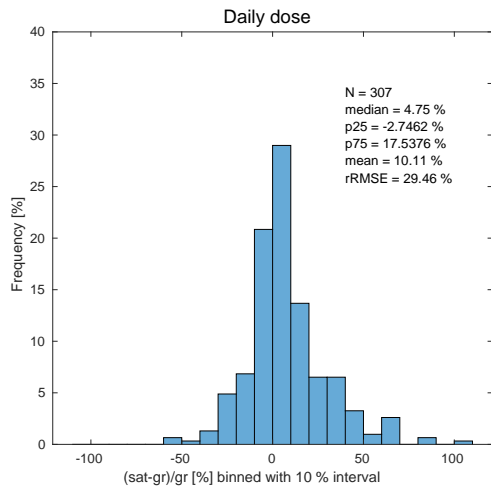
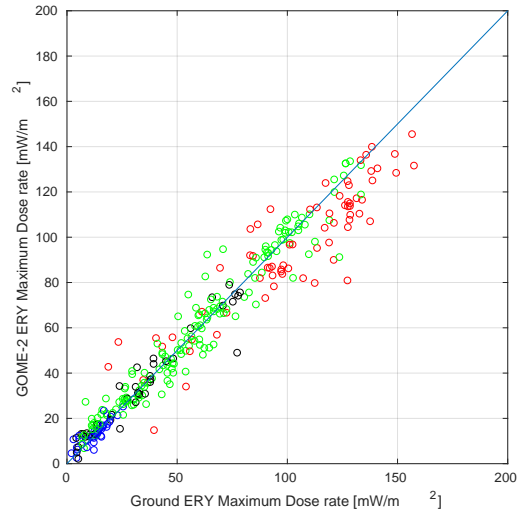
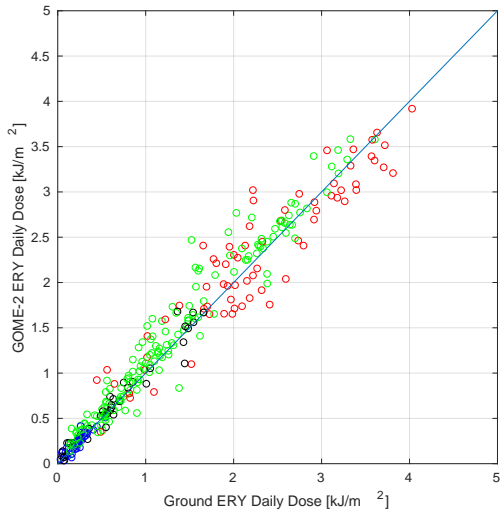


Figure 4: Helsinki

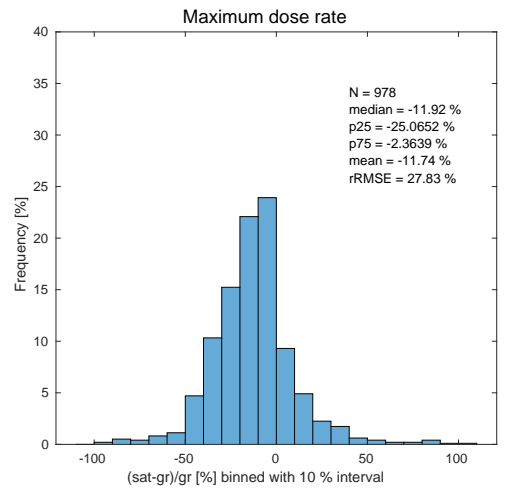
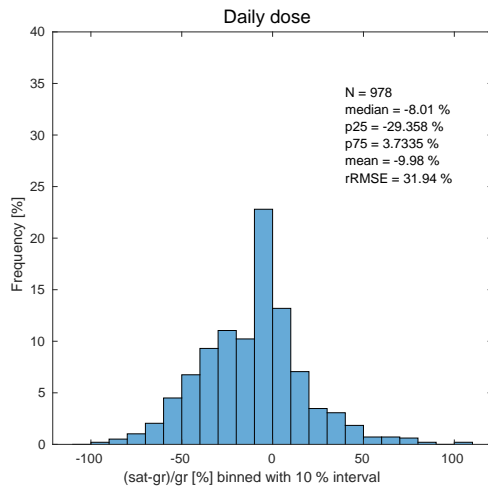
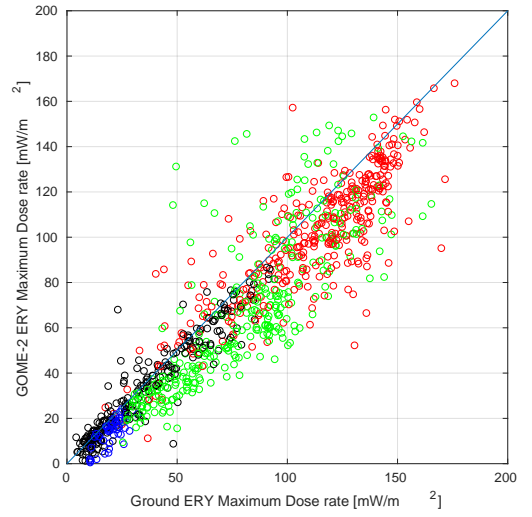
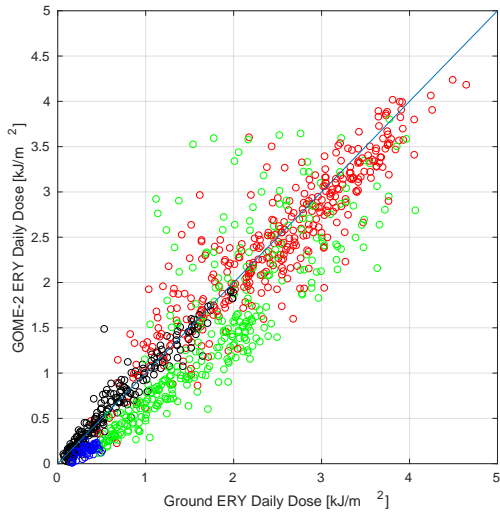


Figure 5: Churchill

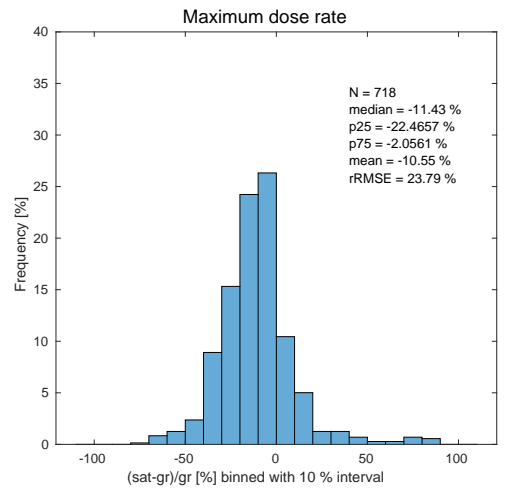
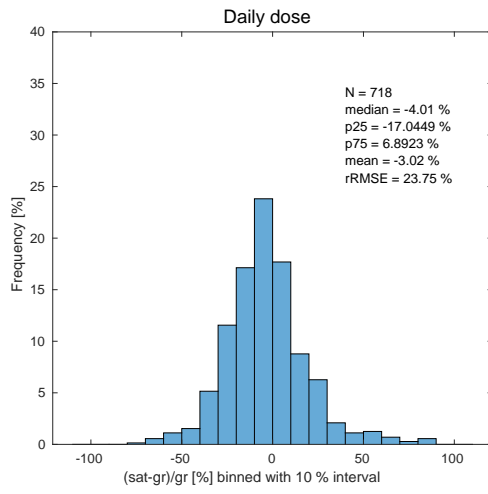
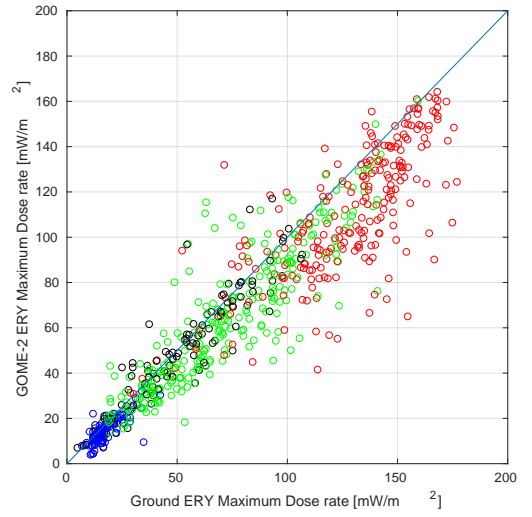
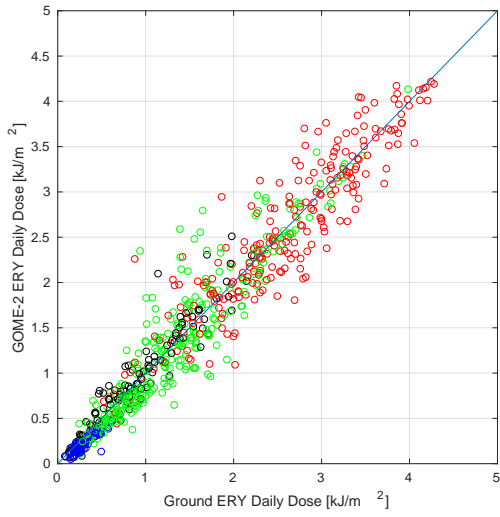


Figure 6: Tomsk

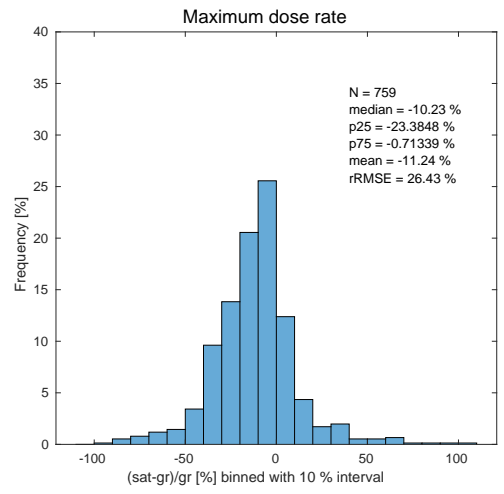
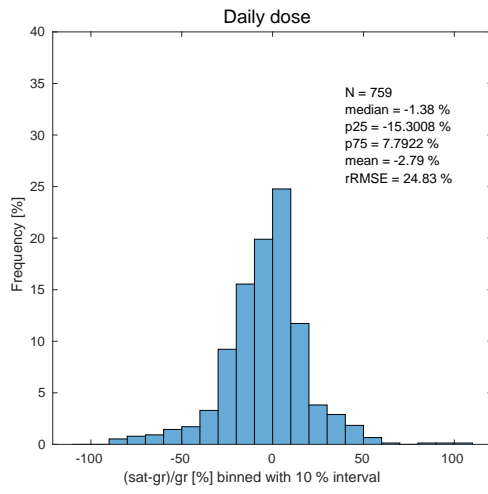
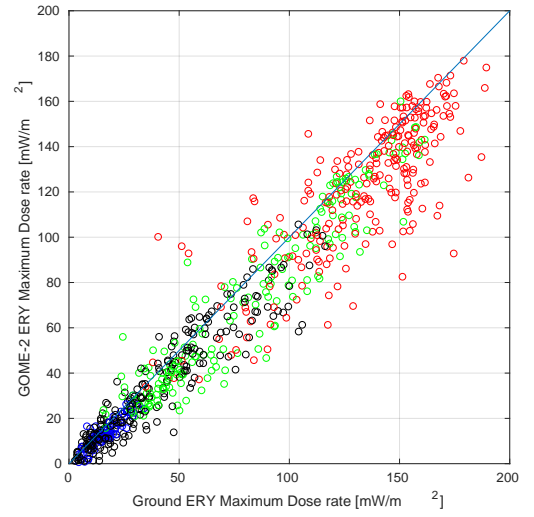
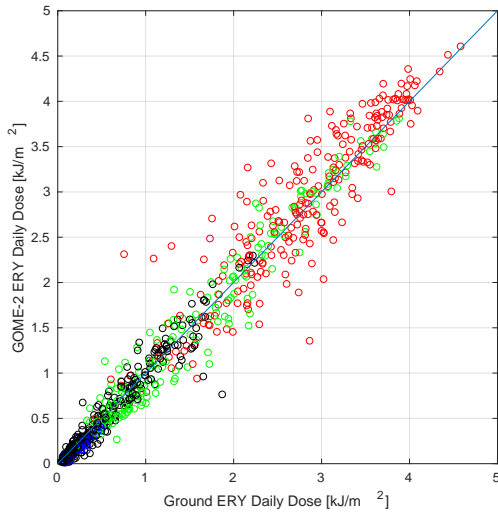


Figure 7: Obninsk

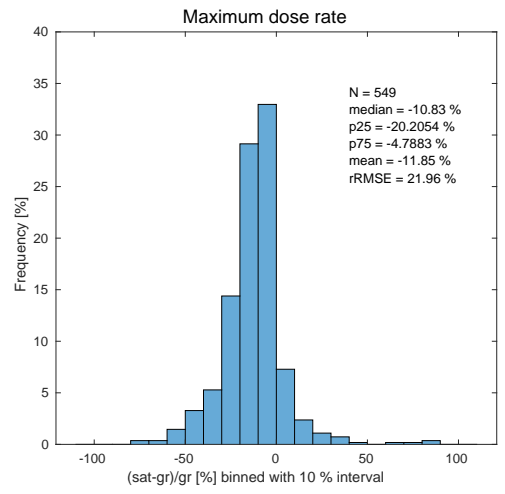
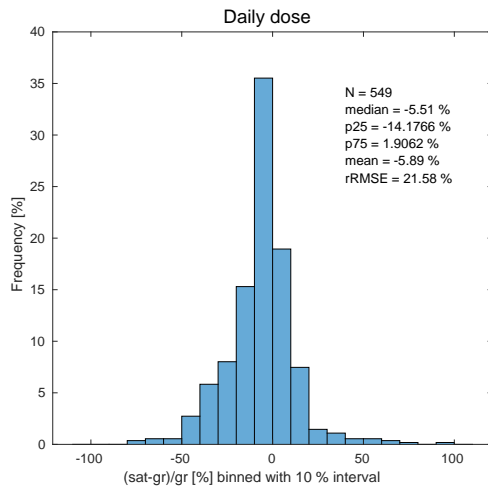
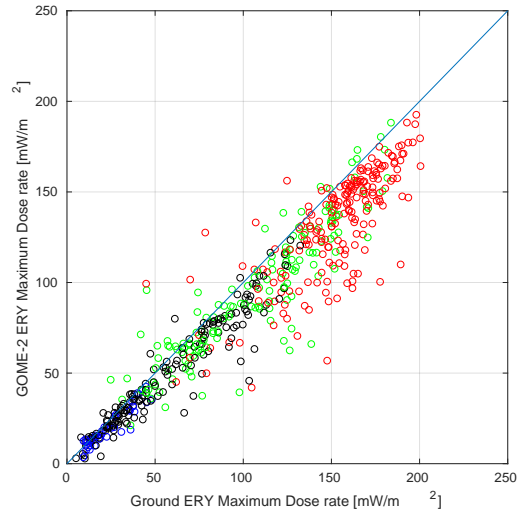
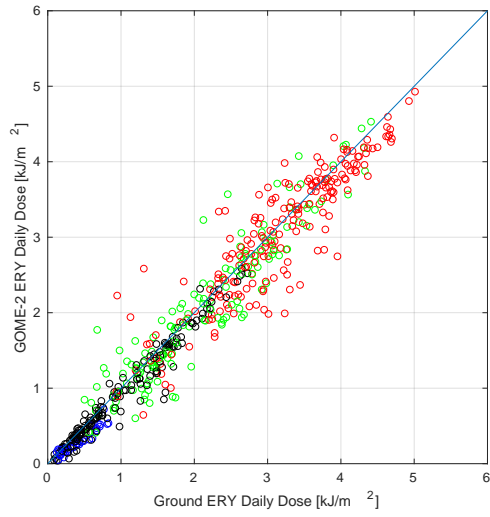


Figure 8: Edmonton

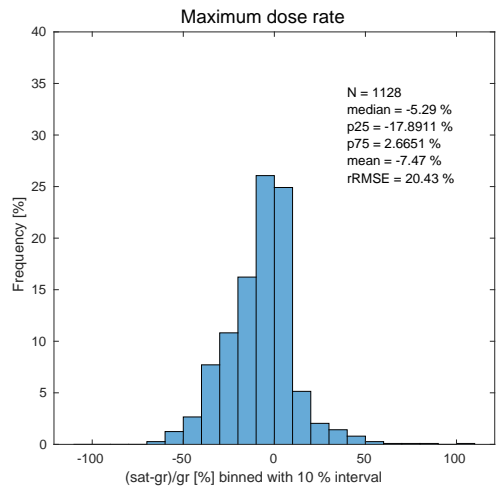
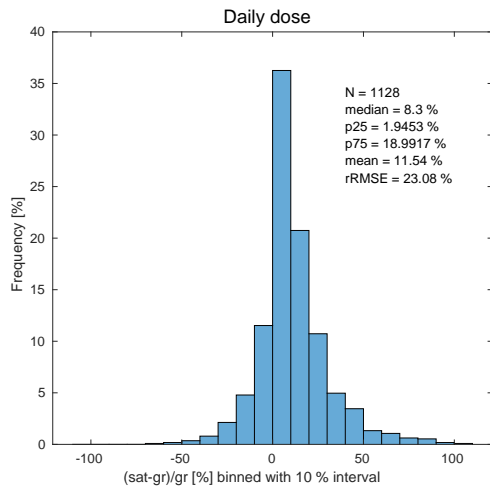
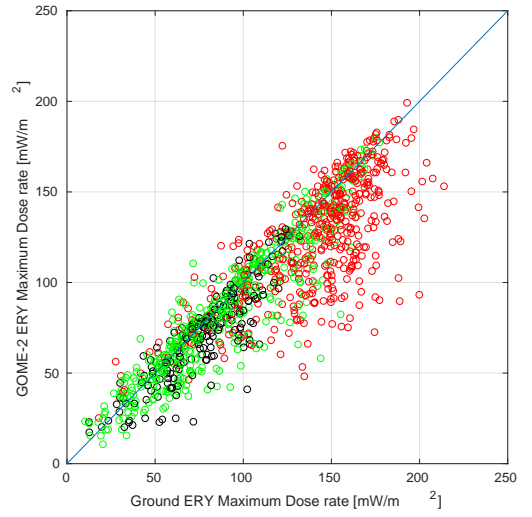
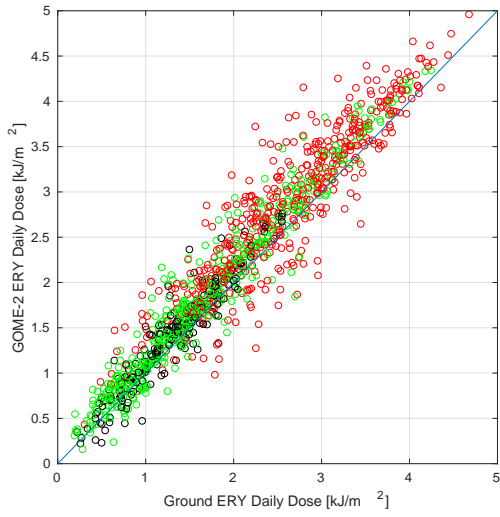


Figure 9: Uccle

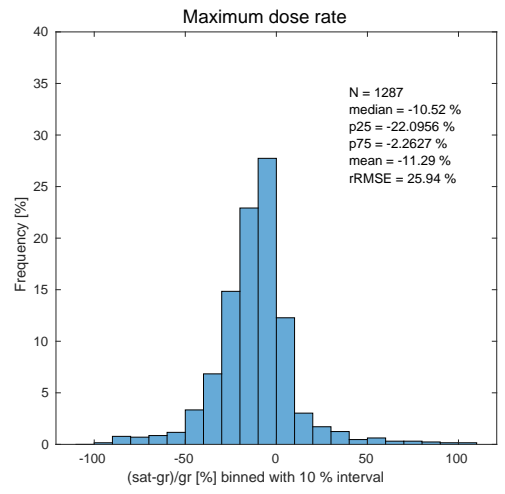
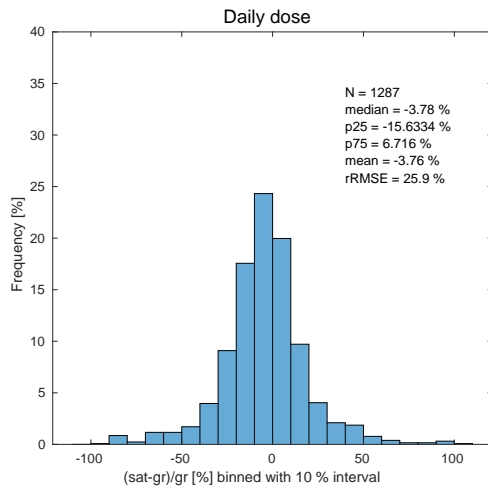
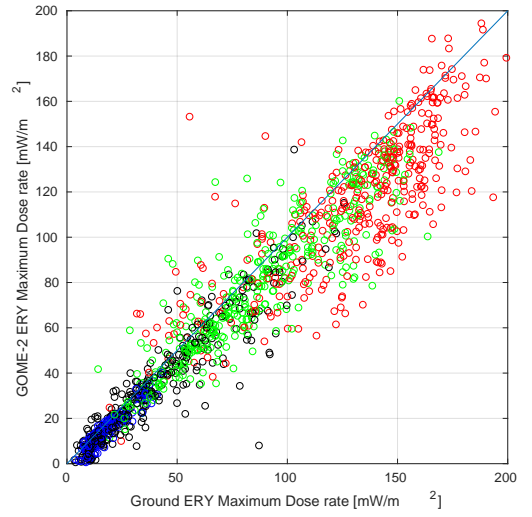
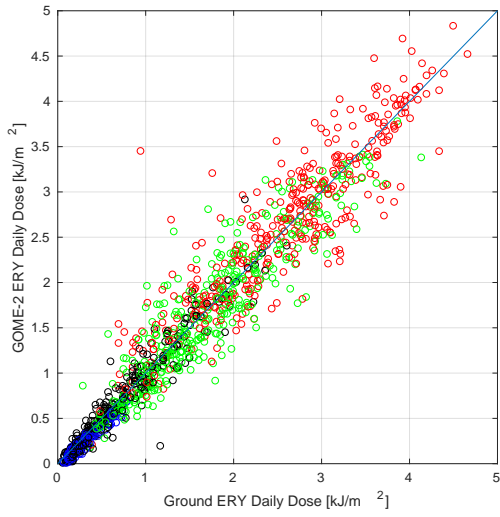


Figure 10: Goose Bay

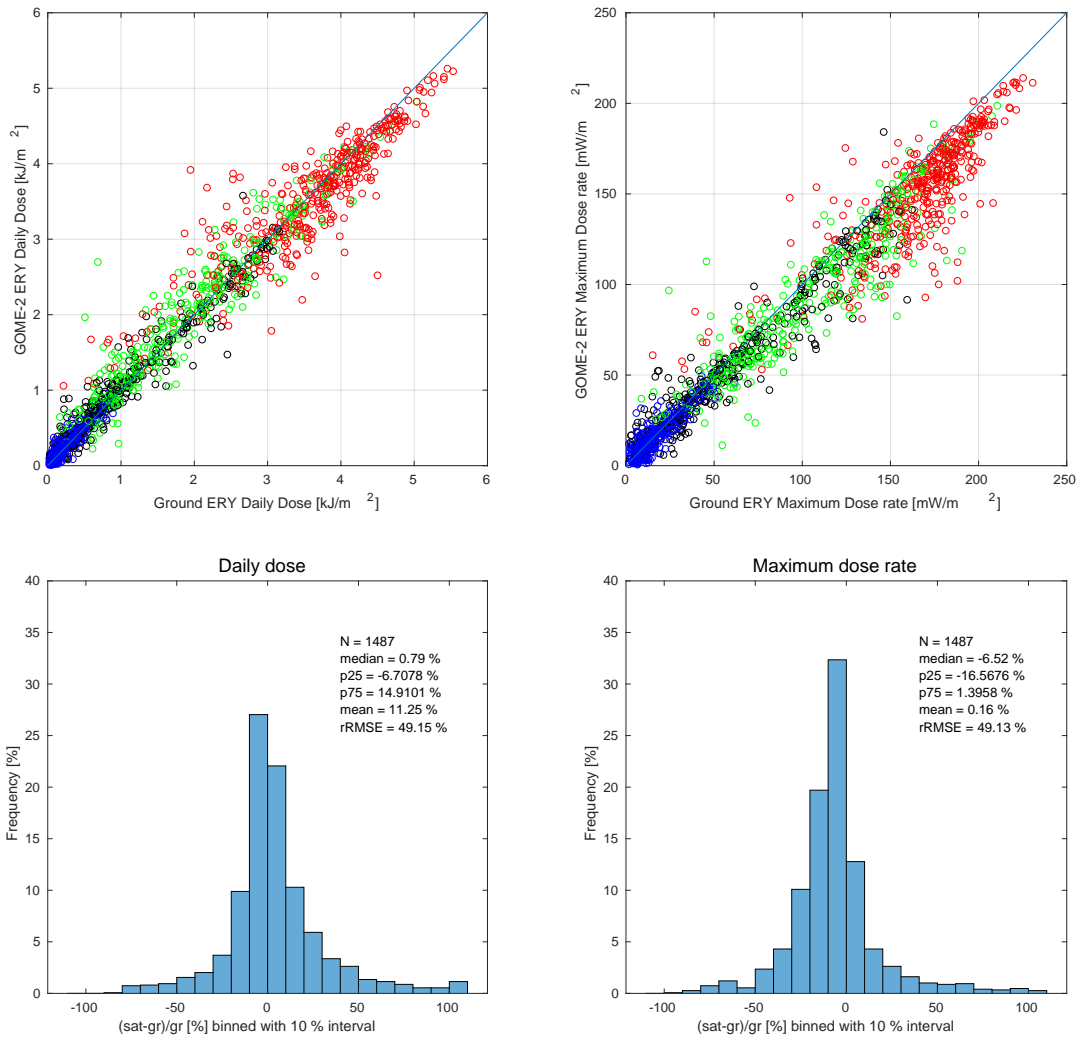


Figure 11: Saturna Island

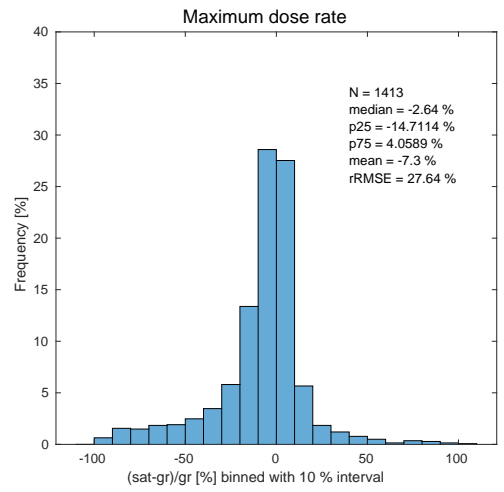
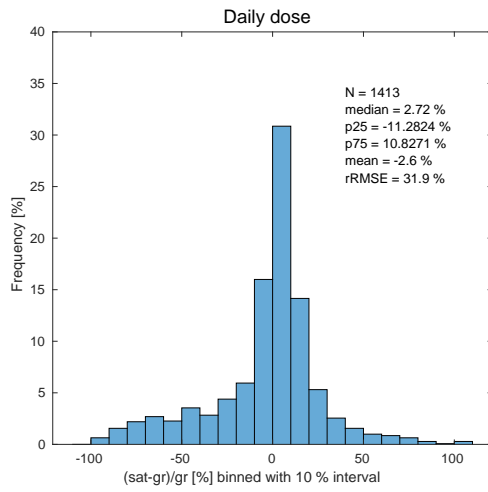
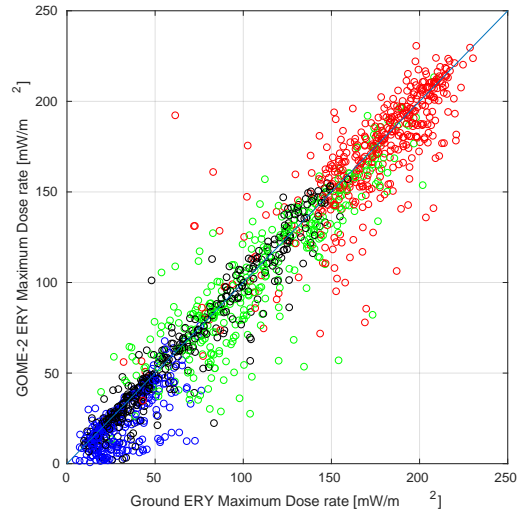
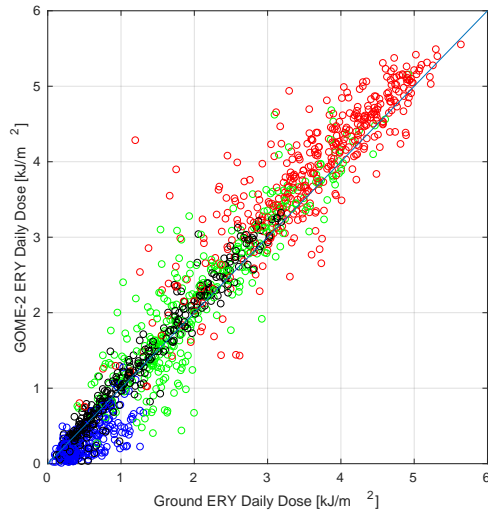


Figure 12: Ft. Peck

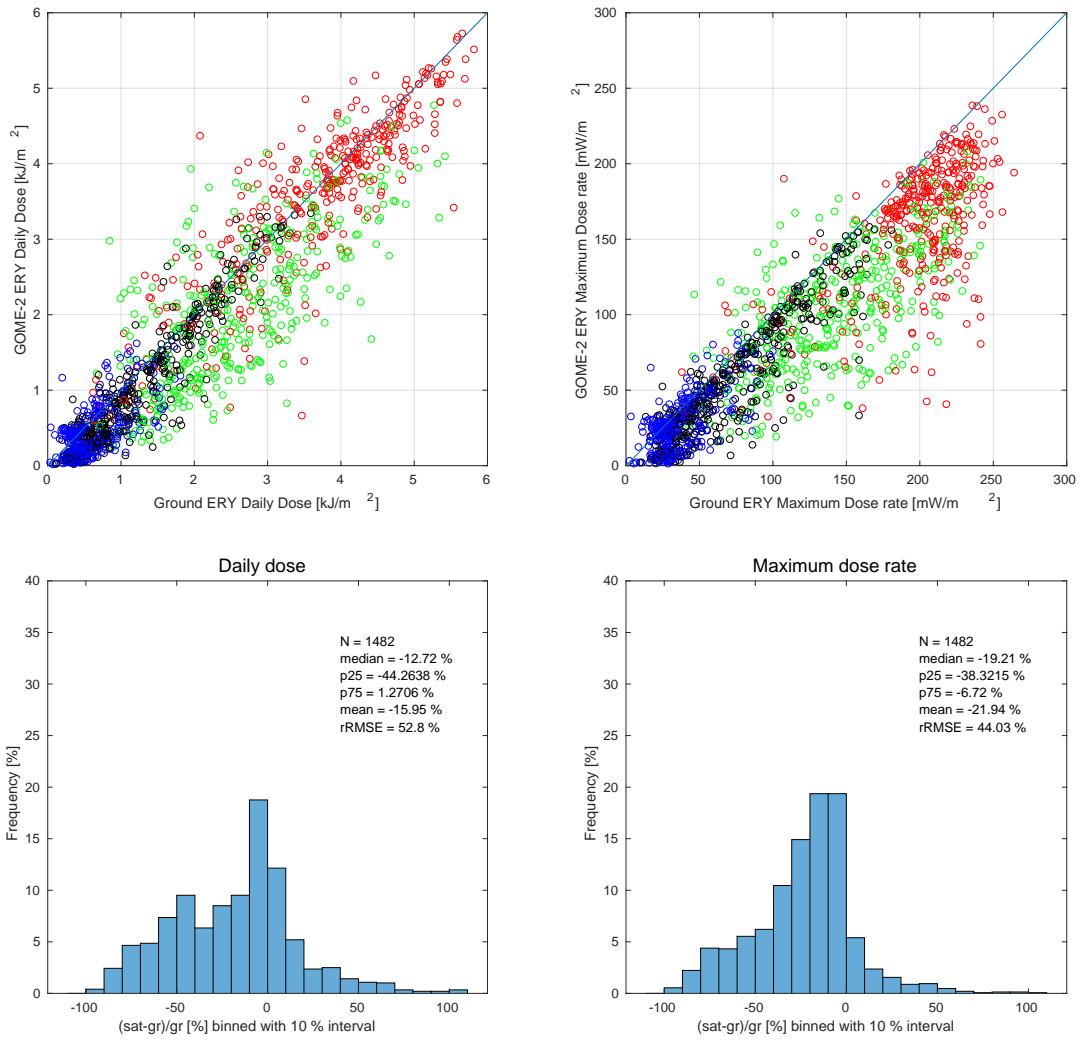


Figure 13: Davos

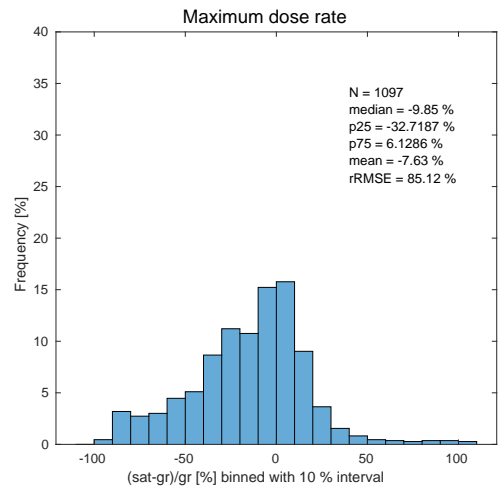
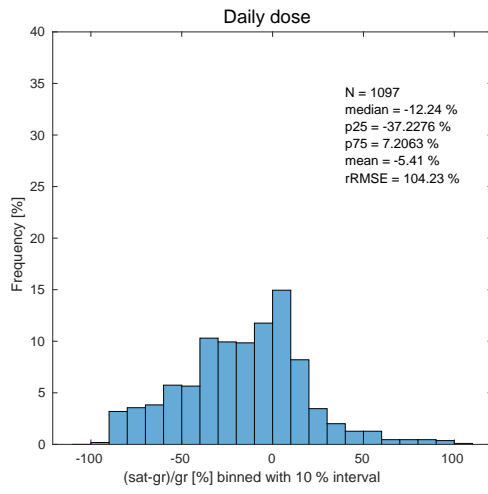
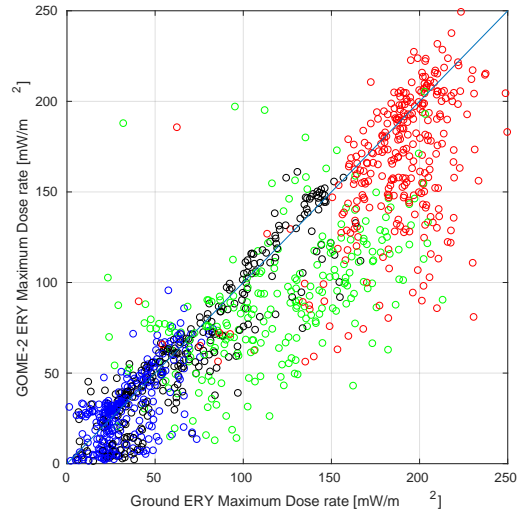
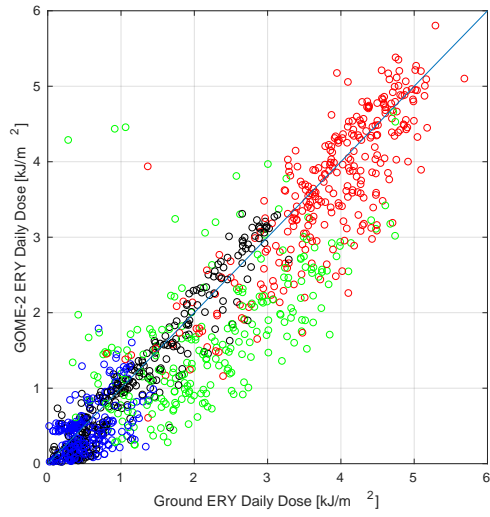


Figure 14: Aosta

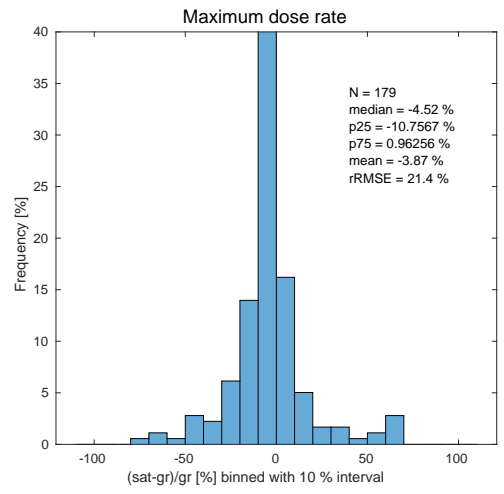
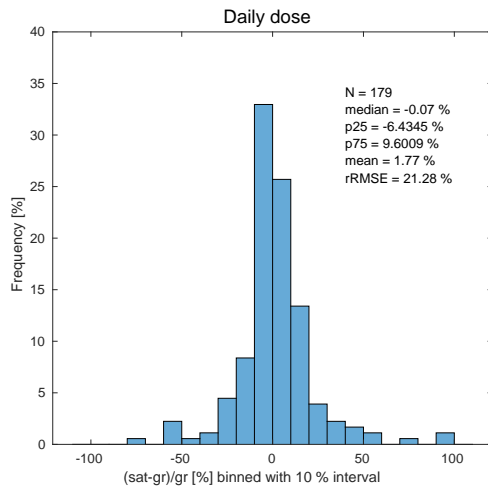
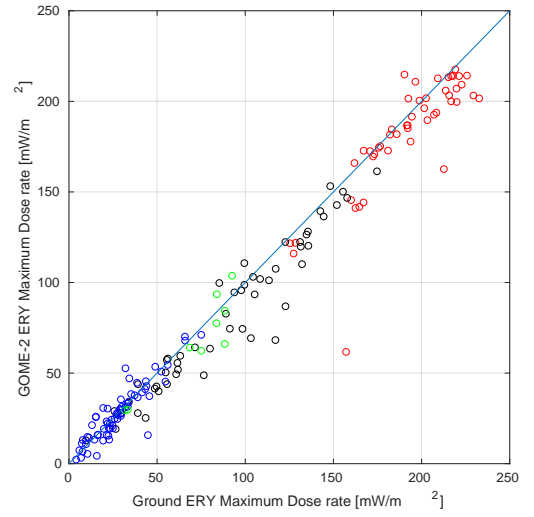
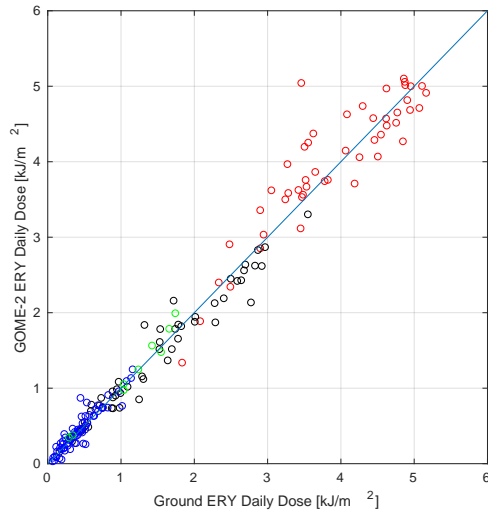


Figure 15: Toronto

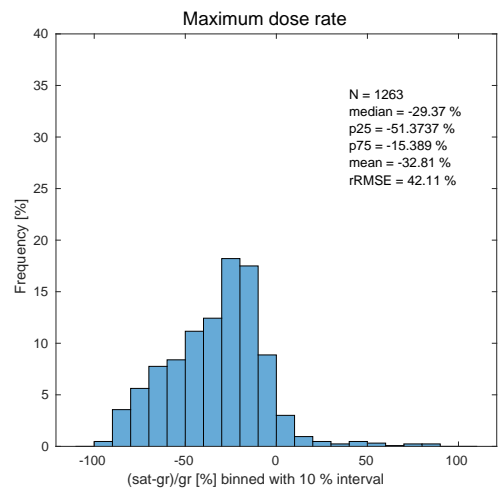
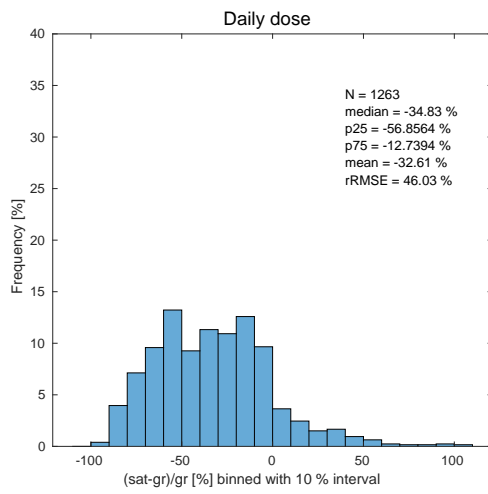
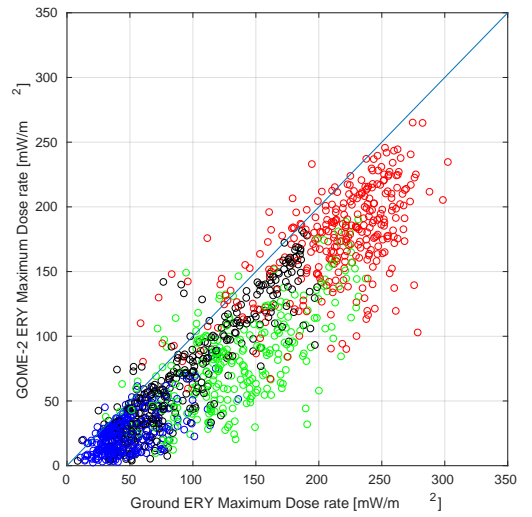
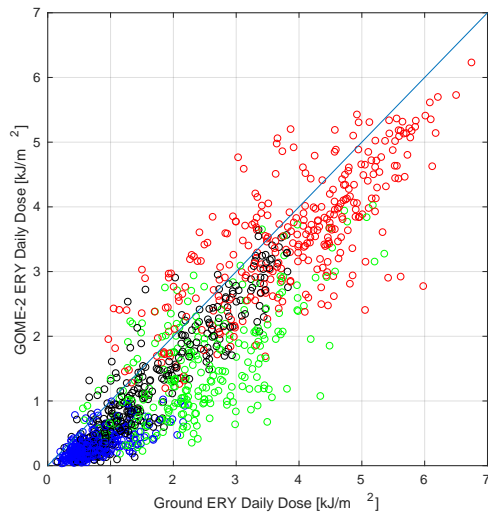


Figure 16: Kislovodsk

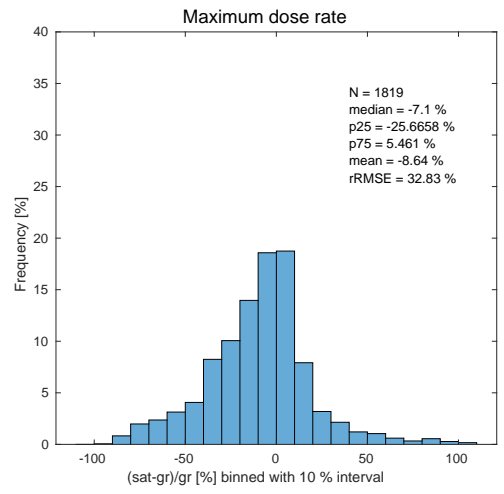
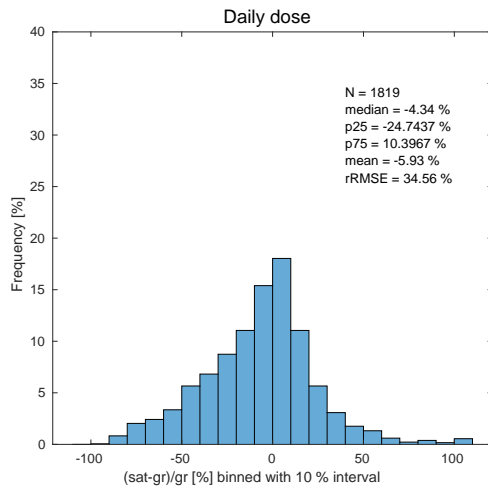
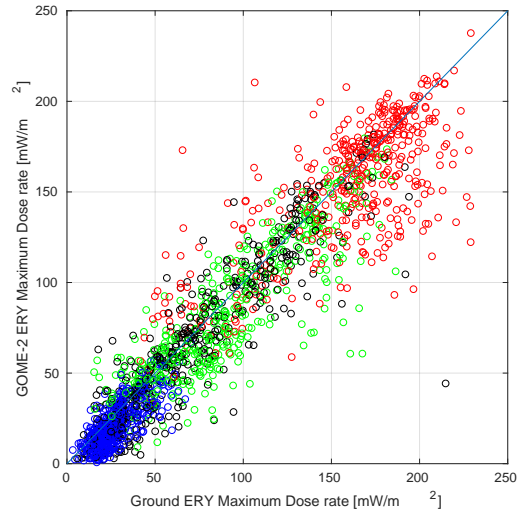
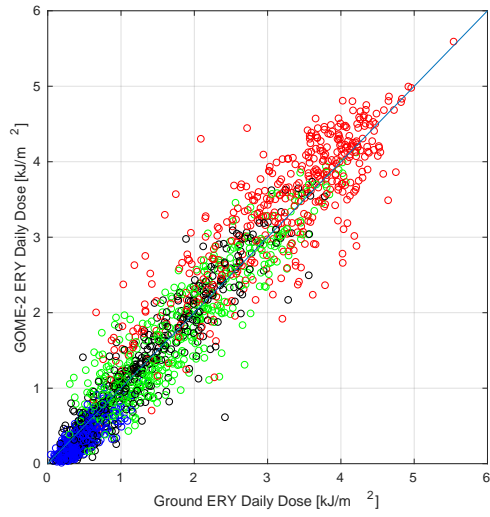


Figure 17: Sapporo

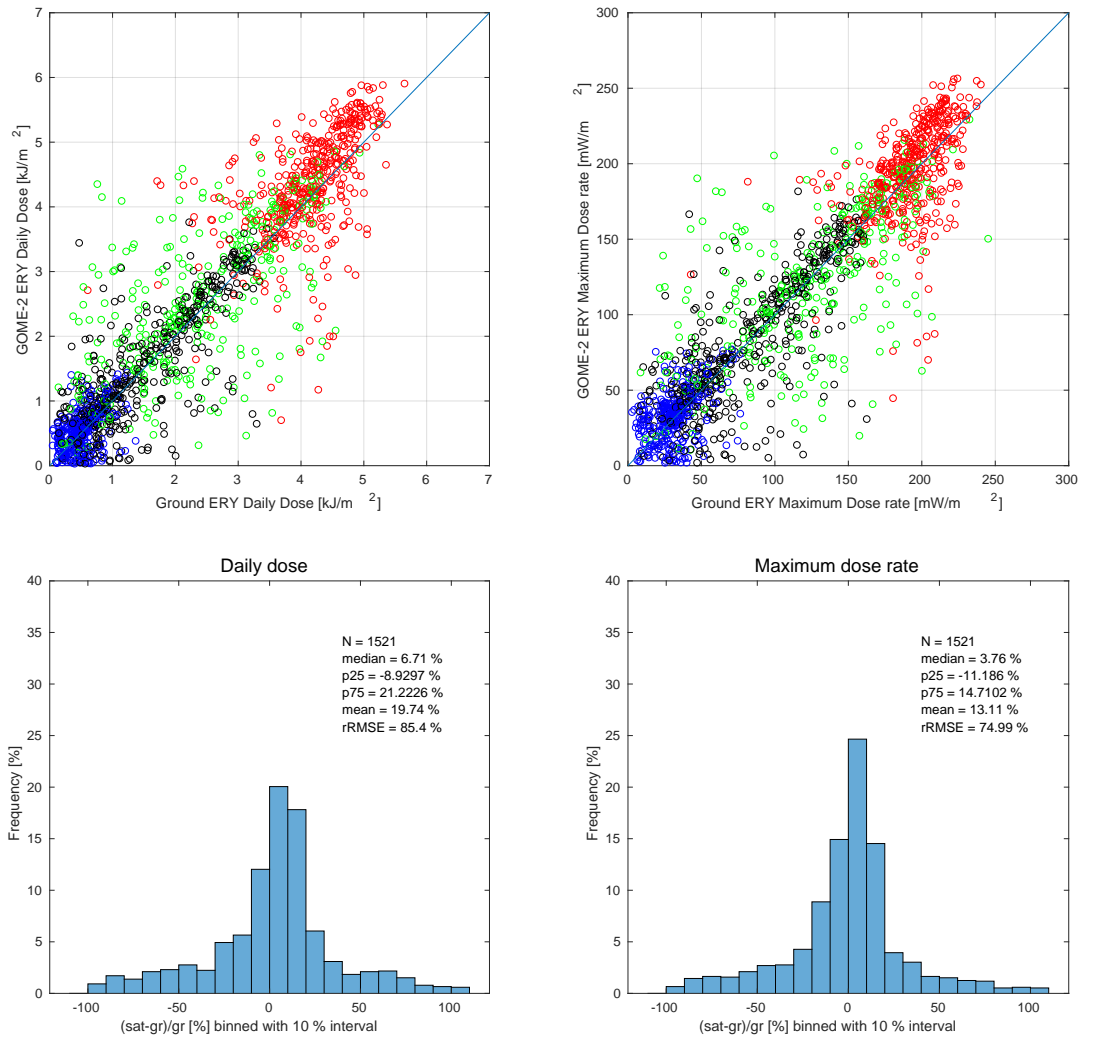


Figure 18: Thessaloniki

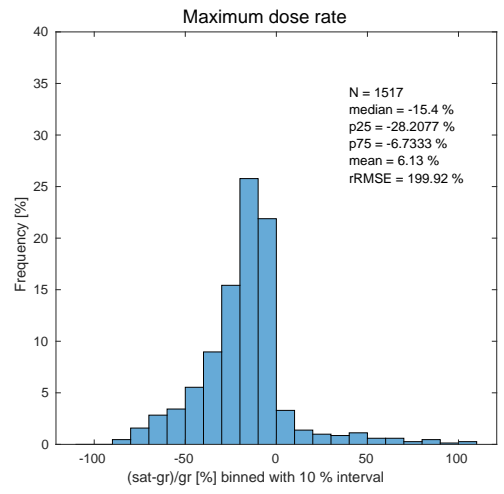
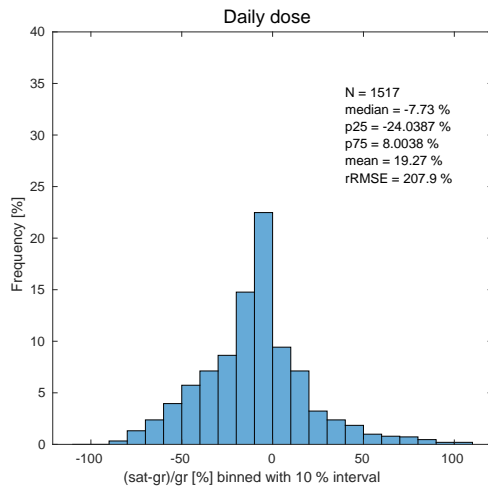
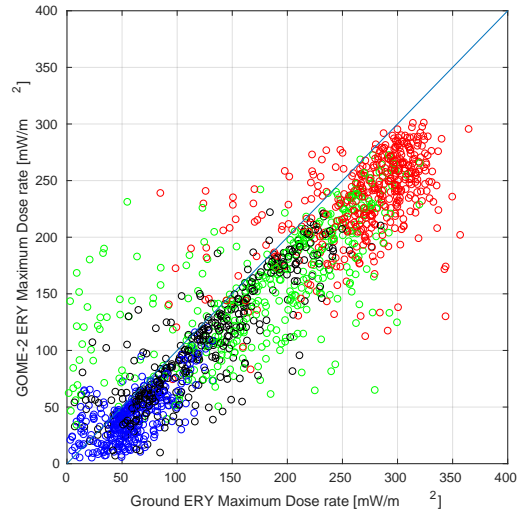
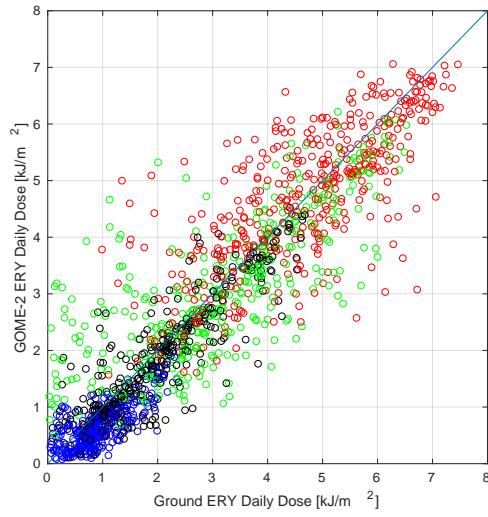


Figure 19: MRS Niwot Ridge

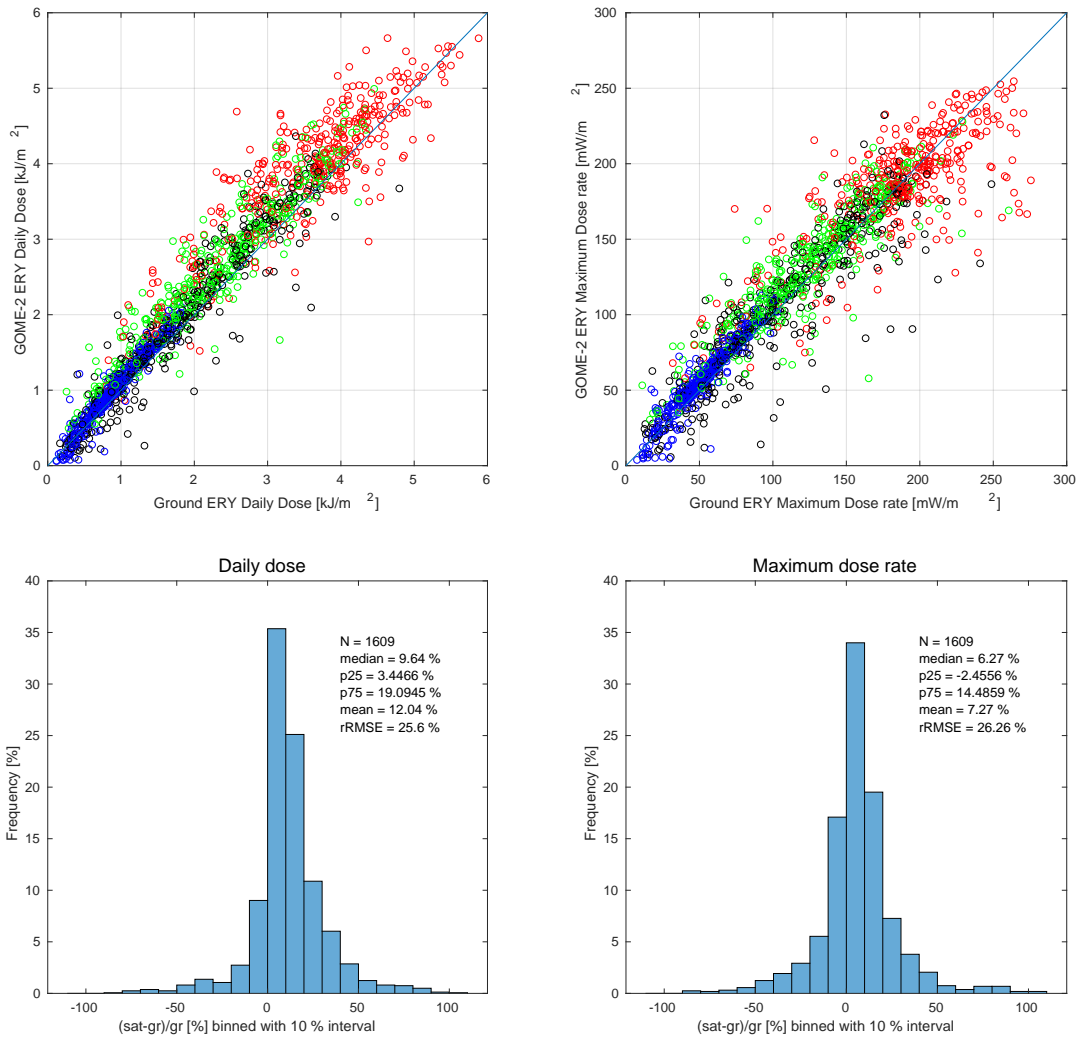


Figure 20: Tsukuba

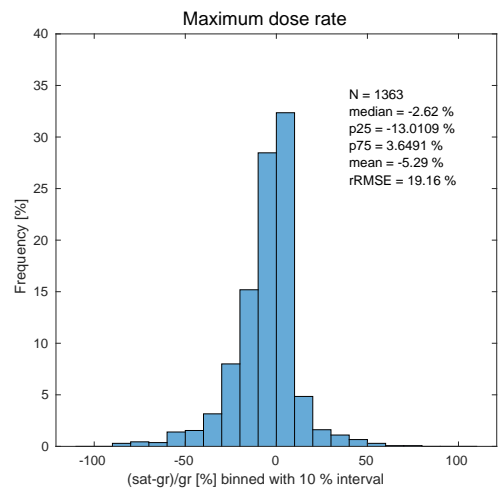
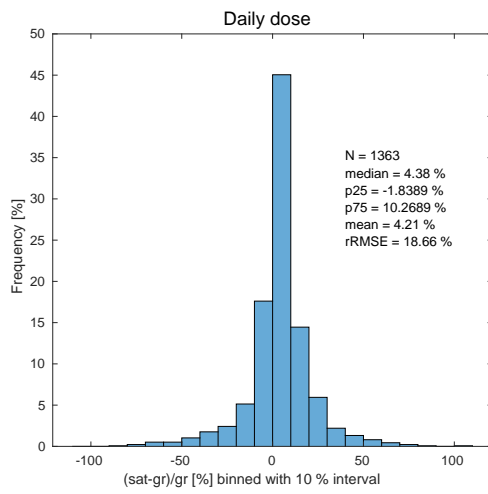
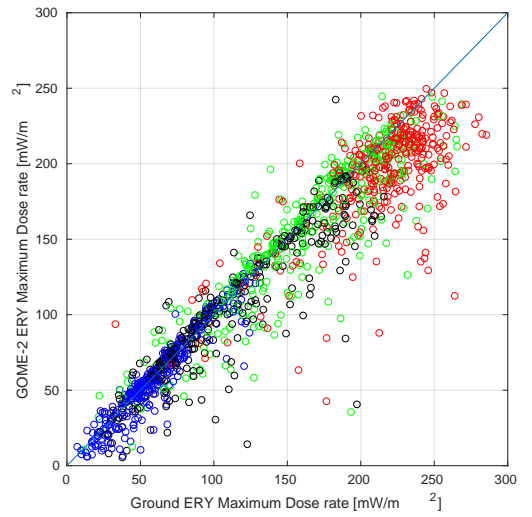
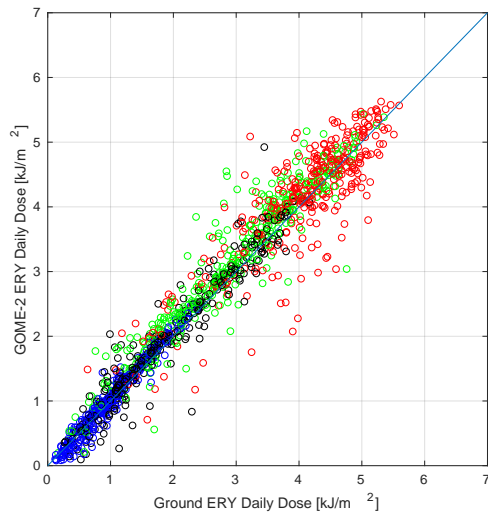


Figure 21: Raleigh

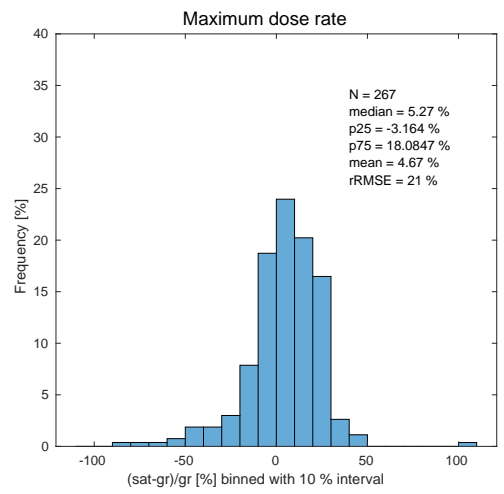
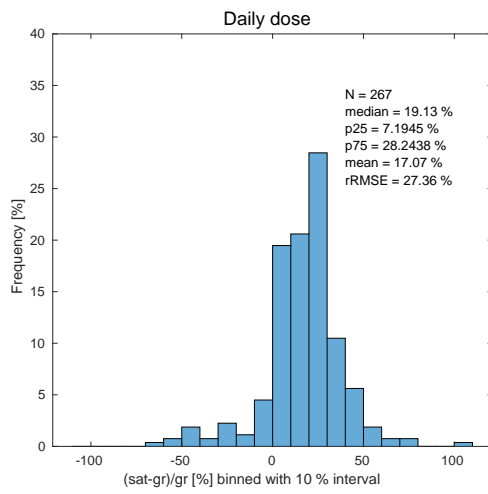
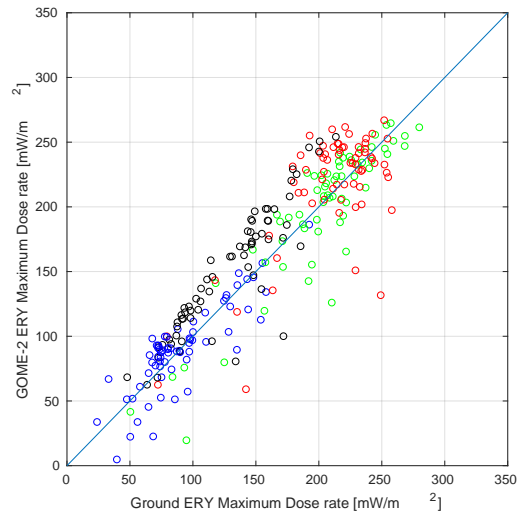
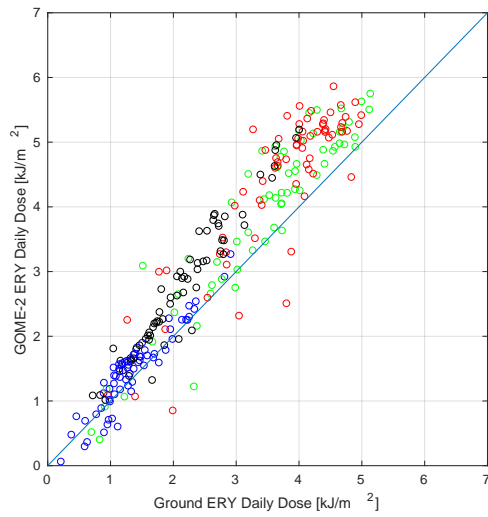


Figure 22: Houston

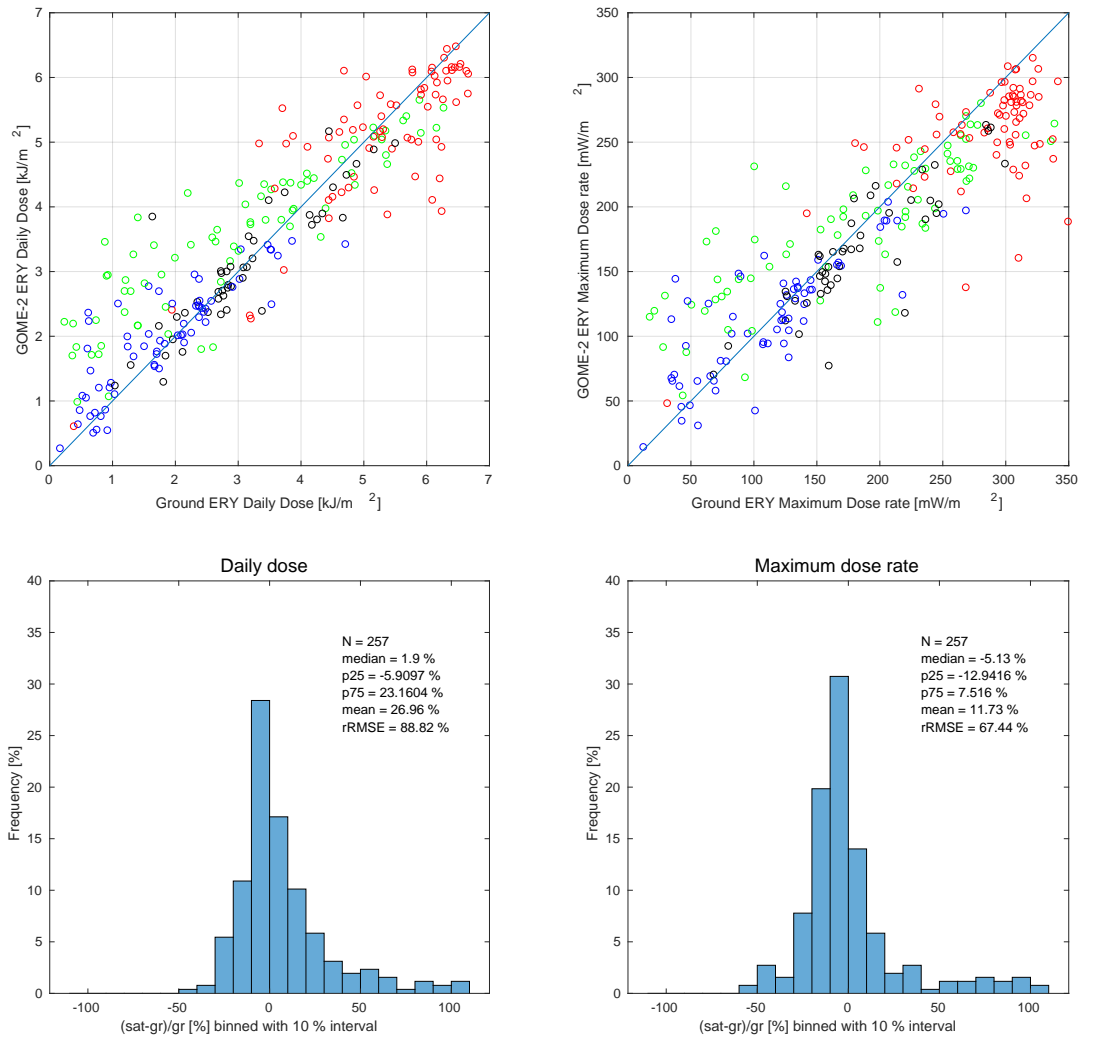


Figure 23: Cape D'Aguilar

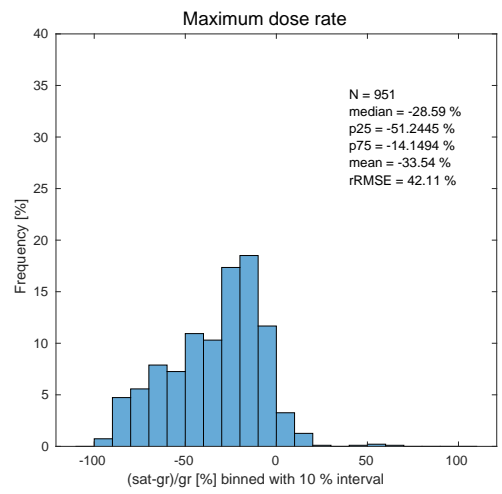
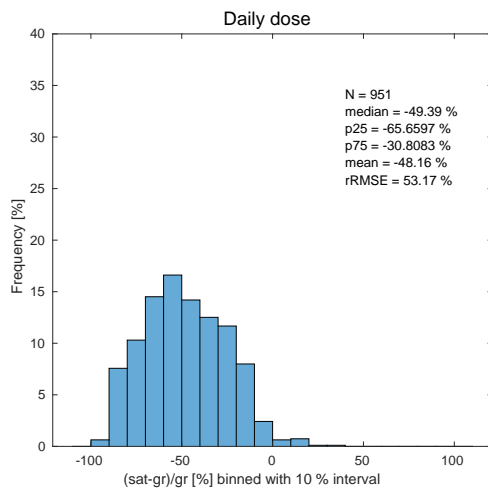
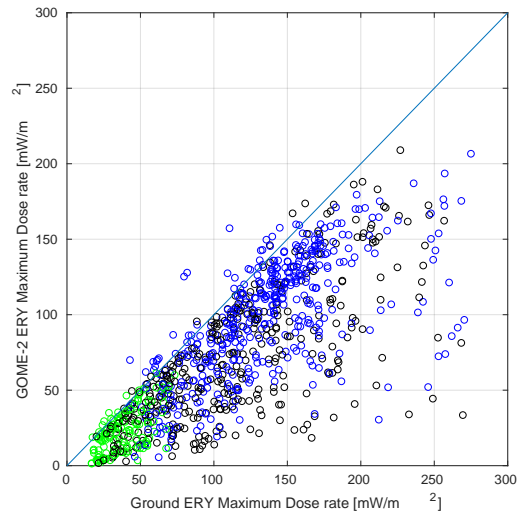
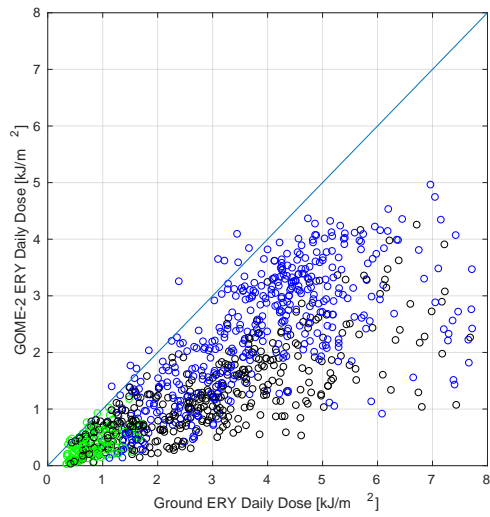


Figure 24: Syowa

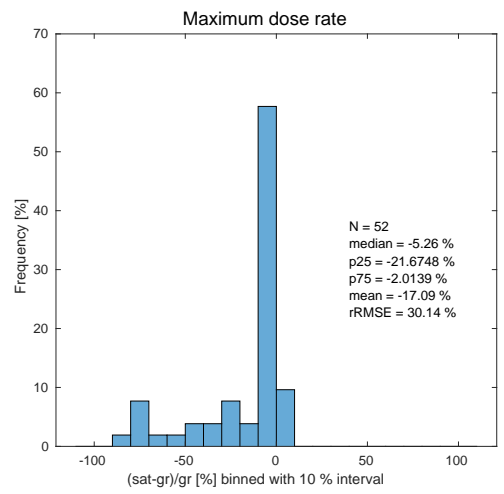
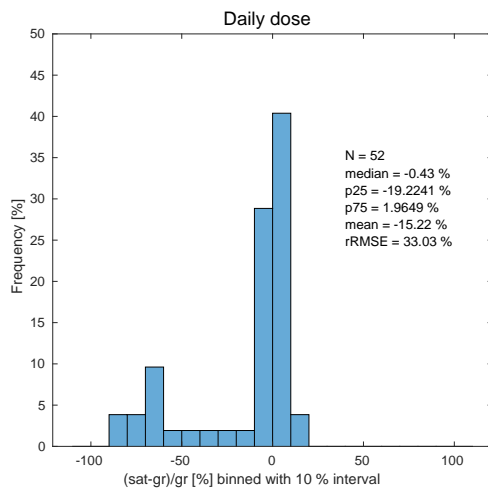
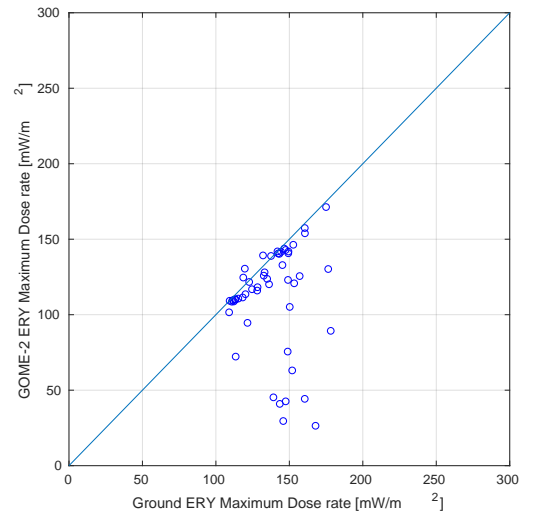
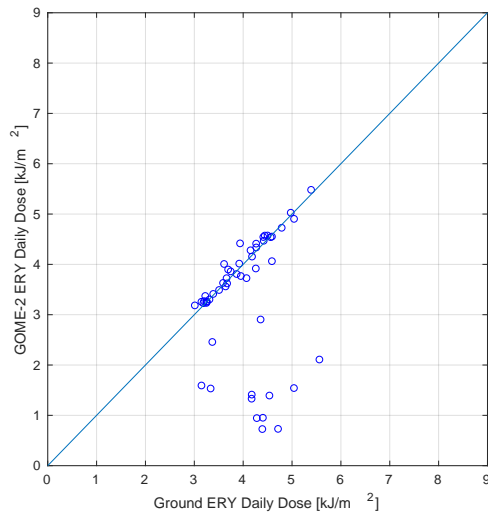


Figure 25: Utsteinen

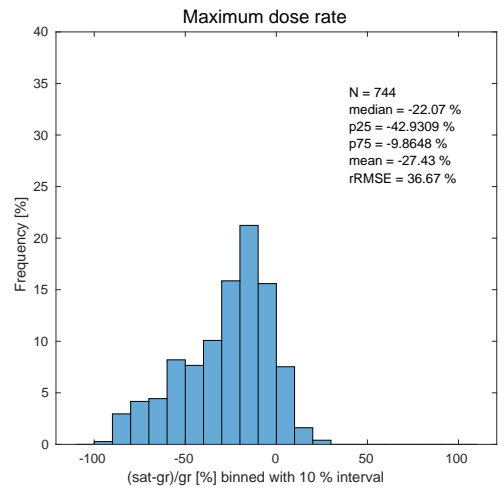
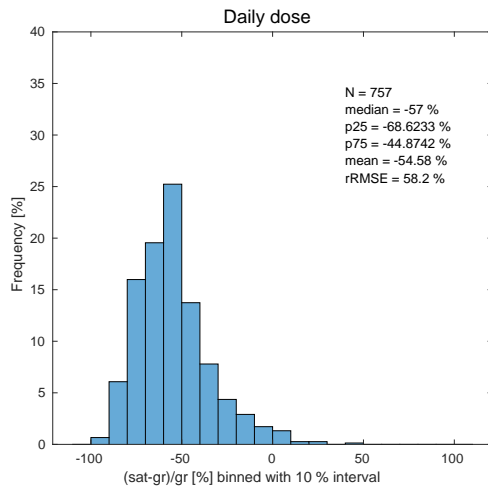
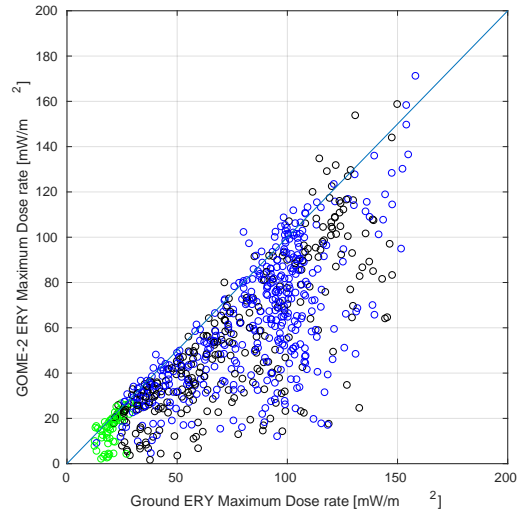
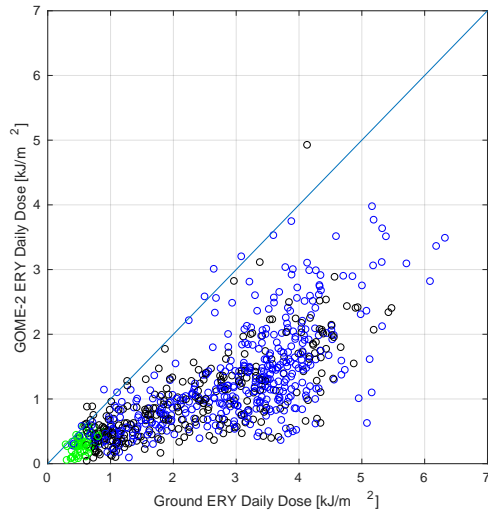


Figure 26: McMurdo